The Effect of Cell Geometrical Design and Hydrodynamic Conditions on the Gas Dispersion of Jameson Cell

Submitted by

Xiangzhou Ding

Department of Mining and Materials Engineering

For the Degree of Master of Engineering

McGill University

Montreal, Canada

Summer, 2016

Supervised by: James A. Finch

Abstract

Through decades of development, the Jameson Cell has become a popular choice of flotation machine in coal, base metal processing and other specialist applications. Its vigorous bubble-generation and the bubble-slurry mixing mechanisms are not yet fully understood. Employing the sensors and bubble viewing techniques now available, this project examined experimentally how the performance of a lab scale Jameson Cell related to design and operating variables. The results are of interest to Jameson Cell operators and modelers. Some of the important findings are: both orifice size and downcomer length positively impact the vacuum in downcomer thus promotes small bubbles and high gas holdup; the higher jet pressure generates smaller bubbles; downcomer length does not have a significant effect on the bubble size.

Résumé

Des décennies de développement ont permis à la Jameson Cell de devenir un dispositif de flottaison populaire dans les domaines du charbon, du traitement des métaux de base et d'autres applications spécialisées. Néanmoins, sa vigoureuse production de bulles et ses mécanismes de mélange bulles-boue ne sont pas encore entièrement compris. Par l'utilisation de capteurs et de techniques de visualisation de bulles les plus récentes, ce travail examine, de façon expérimentale, la façon dont la performance d'une Jameson Cell de laboratoire est reliée aux variables de conception et d'opération. Les résultats de ce travail contribuent au travail des opérateurs et des modeleurs de la Jameson Cell. Certains des résultats importants sont: la taille de l'orifice et la longueur du '*downcomer*' ont un impact positif sur le vide dans le '*downcomer*', cela favorise de petites bulles et la rétention de gaz haute, la pression de jet supérieur génère de petites bulles, la longueur du tuyau de descente n'a pas d'effet significatif sur la taille des bulles.

Acknowledgements

Thanks to all my friends and colleagues in the Mineral Processing Group at McGill University as they offered valuable advice and encouragement during my study.

Special thanks to all the sponsors that have provided funding and support for this project. This work was performed with funding under the NSERC-CRD (Natural Sciences and Engineering Research Council-Collaborative Research and Development) program with the following industrial partners: Vale, Teck, Barrick, SGS Lakefield, XPS, Flottec, and Shell Canada. Key components of the equipment to set up the Jameson Cell at McGill University were provided by Xstrata, and is gratefully acknowledged.

During my work, I was fortunate to receive advice and technical support from some special individuals. Dr. Cesar Gomez, who is an expert in gas dispersion measurements in flotation, offered continuous help on operating equipment. Mr. Armando Navarrete instructed me on bubble sizing techniques. Mr. Jan Nesset gave me practical advice on data management. Prof. Kristian Waters and Mr. Raymond Langlois's enthusiastic collaboration and their technical support are appreciated.

Finally, I would like to thank my supervisor, Professor James A. Finch. Prof. Finch left with me impressions of being brilliant and insightful during my studies at McGill University. Through his teaching from The Introduction to Mineral Processing to courses such as Advance Mineral Processing Systems, I was inspired and took an interest in the field of Mineral Processing. His experience and knowledge provided me guidance and I am grateful.

Table of Contents

Abstract 1

Résumé 2

Acknowledgements 3

List of Figures 6

Chapter 1: Introduction 9

1.1. Brief Introduction to Jameson Cell 9

1.2. Thesis Objective 11

Chapter 2: Theoretical Background 12

2.1. Jameson Cell Design 12

2.1.1. Industrial Jameson Cell 13

2.1.2. Jameson Cell Development 15

2.2. Background of Jameson Cell 20

2.2.1. Principles of Operation 20

2.2.2. Prediction of Bubble Size Generated by Plunging Liquid Jet Reactor 25

2.3. Operating Conditions and Controlled Variables in Jameson Cell 28

2.3.1. Primary Variables 28

2.3.2. Secondary Variables 30

2.3.3. Jameson Cell Particle Collection Mechanisms 37

Chapter 3: Experimental Apparatus 39

3.1. Jameson Cell Developed at McGill University 39

3.2. Data Acquisition Techniques 42

Chapter 4. Experimental Procedures and Sample Calculations 47

4.1. General Procedure 47

4.2. Bubble Sizing Technique 48

4.2.1. Bubble Size Data Management 48

4.2.2. Bubble Sizing Method 50

4.3. Pressure and bubble size correction 54

Chapter 5: Results and Discussion 56

5.1. Vacuum Pressure and Working Condition of Downcomer 56

5.1.1. The effect of flowrate on vacuum pressure 56

5.1.2. The Effect of Orifice Size on Vacuum Pressure 58

5.1.3. The Effect of Downcomer Length on Vacuum Pressure 61

5.1.4. The Effect of Frother Concentration on Vacuum Pressure 63

5.2. Jet pressure of Jameson Cell Downcomer 64

5.3. Tank Gas Holdup 65

5.4. Bubble Size 68

5.4.1. The Effect of Aeration Rate on Bubble Size 68

5.4.2. The Effect of Water Flowrate on the Bubble Size and Its Implications 69

5.4.3. The Effect of Frother on the Bubble Size 71

5.4.4. The Effect of Jameson Cell Geometry on the Bubble Size 75

Chapter 6: Conclusions and Future Work 77

References 79

List of Figures

Figure 1: Schematic of Jameson Cell 13

Figure 2: Schematic of industrial Jameson Cell 14

Figure 3: Wash water system in Jameson Cell for coal flotation 15

Figure 4: Downcomer developments from 1994-1999 18

Figure 5: Schematic of slurry lens for Mark III and Mark IV downcomer 19

Figure 6: Schematics of Mark III and Mark IV downcomers 20

Figure 7: Hydrodynamic zones of a plunging liquid jet reactor 21

Figure 8: The mechanisms of air transport by a free jet 22

Figure 9: Plunging jet illustration 23

Figure 10: Flow regimes in a plunging jet bubble column 24

Figure 11: Comparison between predicted and measured maximum bubble diameter 28

Figure 12: Variables in Jameson Cell operation 29

Figure 13: Variables of Jameson Cell operation 29

Figure 14: Variation of free jet length 31

Figure 15: The effect of jet length on recovery in the downcomer 32

Figure 16: Concentrate solids production rate vs. froth depth 33

Figure 17: Bubble size as a function of Jg for different flotation machines 34

Figure 18: Gas holdup in Jameson Cell downcomer response to jet velocity under different setups 36

Figure 19: Schematic of the laboratory Jameson Cell 40

Figure 20: Jameson Cell apparatus at McGill – downcomer illustration 41

Figure 21: Sensor Deployments 42

Figure 22: NOSHOK pressure transmitters 43

Figure 23: Magnetic flowmeter 44

Figure 24: Schematic illustration of McGill Bubble Viewer 46

Figure 25: A sample of bubble size frequency of a bubble collection 50

Figure 26: Sample bubble picture, original 51

Figure 27: Sample bubble picture, contrast threshold applied 52

Figure 28: sample bubble picture, bubbles recognized and counted 53

Figure 29: Bubble size correction calculation 55

Figure 30: APR vs. vacuum pressure in an operating downcomer 57

Figure 31: Contour diagram of APR effect on vacuum pressure 58

Figure 32: Contour diagram of APR effect on Vacuum Pressure: 4mm orifice 59

Figure 33: Contour diagram of APR effect on Vacuum Pressure: 5mm orifice 60

Figure 34: Contour diagram of APR effect on Vacuum Pressure: 6mm orifice 60

Figure 35: Effect of downcomer length on vacuum pressure 62

Figure 36: Frother effect on the vacuum pressure in downcomer 63

Figure 37: The effect of orifice size on the jet pressure 64

Figure 38: The effect of downcomer length on the jet pressure 65

Figure 39: Gas holdup in separation tank is related to Jg and vacuum pressure 67

Figure 40: The effect of frother conc. on the tank gas holdup 67

Figure 41: The effect of air flowrate on bubble size in Jameson Cell 69

Figure 42: The effect of water flowrate on bubble size in Jameson Cell 70

Figure 43: Flowrate vs. bubble size (under APR=1 condition) 71

Figure 44: Bubble size profile: 5ppm frother 72

Figure 45: Bubble size profile: 10ppm frother 73

Figure 46: Bubble size profile: 15ppm frother 73

Figure 47: Bubble size profile: 30ppm frother 74

Figure 48: Bubble size profile: 60ppm frother 74

Figure 49: Comparison of bubble size generated by long and short downcomer 76

Chapter 1: Introduction

1.1. Brief Introduction to Jameson Cell

Froth flotation, one of the most commonly used techniques for mineral separation, has been in use for over a century. It takes advantage of the difference in surface properties of minerals to achieve the separation of valuable minerals from non-valuable minerals, or gangue. Numerous flotation device have been invented and can be classified into two groups: pneumatic and mechanical machines [1]. Such classification is based on the mechanism of bubble introduction into the flotation cell. Mechanical machines disperse air into small bubbles with mechanically driven impellers; pneumatic machines, on the other hand, introduce air through other means such as turbulent entrainment, and spargers. The most common pneumatic device today is the flotation column. A development in column-type flotation machines into a more compact device (smaller height), resulted in the Jameson Cell [2].

The Jameson Cell disperses air into slurry together in a vertical tube ("downcomer"), to create the flotation environment. The discharge from the downcomer is into a tank where the particle-loaded bubbles disengage from the slurry to rise and form a froth ("separation tank"). The development originated from the concept of the Plunging Liquid Jet Reactor, patented in 1907 [3]. In the patent Norris notes that "the air appears to be dissolved and entrained into a stream pulp" [3]. Flotation devices that entrain air using a plunging liquid jet were generally referred to as "cascade machines" and formed the background that that lead to the invention of Jameson Cell[4].

In 1986, Mount Isa Mines Ltd. introduced large flotation columns in the copper and lead/zinc circuits [5]. Through the use of wash water introduced into the froth a higher

grade float product (concentrate) was produced than the prior mechanical cell technology in place. But flotation columns have slow particle collection rate requiring large residence time (i.e., large cell volume). In the drive to make the design more compact, cell prototypes were devised in the laboratory of Professor Jameson at Newcastle University, Australia, to become the “Jameson Cell”. Air (bubble)/slurry mixing in a vertical tube, the downcomer, was introduced to accelerate particle collections which greatly reduced cell volume, with retention times in seconds for particle collection in the downcomer compared with minutes in the column. By retaining the wash water feature the new cell maintained the advantage of the high grade float product of the columns. The prototypes were tested at Mt. Isa, where Jameson Cells were subsequently installed. They are now widely seen in coal washeries as well as in cleaning duties in base metal operations [6].

According to Xstrata Technology (distributors of the Jameson Cell), by 2013 there were some 320 Jameson Cell units installed worldwide, with almost half in coal operations and a third in base metal flotation such as lead, zinc and copper [7]. A specialized application is oil droplet removal (de-oiling) from solvents in solvent extraction/electrowining plants, and from other effluents in industries as diverse as petroleum, to food processing.

The Jameson Cell has some advantages over mechanical cells and columns. The bubble generating mechanism does not require moving parts and is capable of creating the necessary small bubbles for flotation (ca. 0.5-2.5mm diameter). The Cell provides intense bubble-particle contacting due to the vigorous air/slurry mixing in the downcomer that lowers the residence time giving a high capacity for a given footprint and fast response to

process control variables. The Jameson Cell is easy to maintain because of its lack of moving parts.

The self-aspiration aspect, while simple, does make for an operational challenge: the air rate depends on slurry flowrate and pulp density and level in the separation chamber. This requires a setup that maintains constant volumetric feed rate to the downcomer, sometimes achieved by recycling part of the tailings from the Cell, and effective pulp level control. From a fundamental perspective, the complexity of the fluid dynamics at high Reynolds number characteristic of the downcomer operation, is beyond current computational capacity to model.

1.2. Thesis Objective

To conduct an experimental study to determine the dependence of output gas dispersion variables, gas holdup and bubble size, on design and operating variables

Chapter 2: Theoretical Background

2.1. Jameson Cell Design

The Jameson Cell consists of two main components: the vertical tubes (downcomers) that provide self-aspiration and intense bubble-particle contact, and a tank (separation tank) where particle-bubble aggregates separate from the pulp. Figure 1 is a general schematic. The feed at elevated pressure, is delivered through a nozzle or an orifice plate producing a slurry jet. The descending jet entrains air and as the jet hits the liquid surface the resulting turbulence disperses the entrained air into bubbles. By entraining air the action of the jet generates negative pressure inside the downcomer which both aspirates air and supports the bubble-slurry mixture (i.e., a low density fluid) level in the downcomer. To maintain the level in the downcomer means the air aspiration has to be throttled to retain sufficient negative pressure while still aspirating sufficient air to achieve target flotation rate. As the aerated slurry exits the downcomer into the separation tank, particles attached to bubbles (i.e., hydrophobic particles) are carried upwards into the froth and overflow into the concentrate launder with unattached particles (typically gaugue) exiting as “underflow”

from the separation tank to form the tailing stream. Commonly, a wash water system above the froth is installed to reduce particle entrainment into the froth.

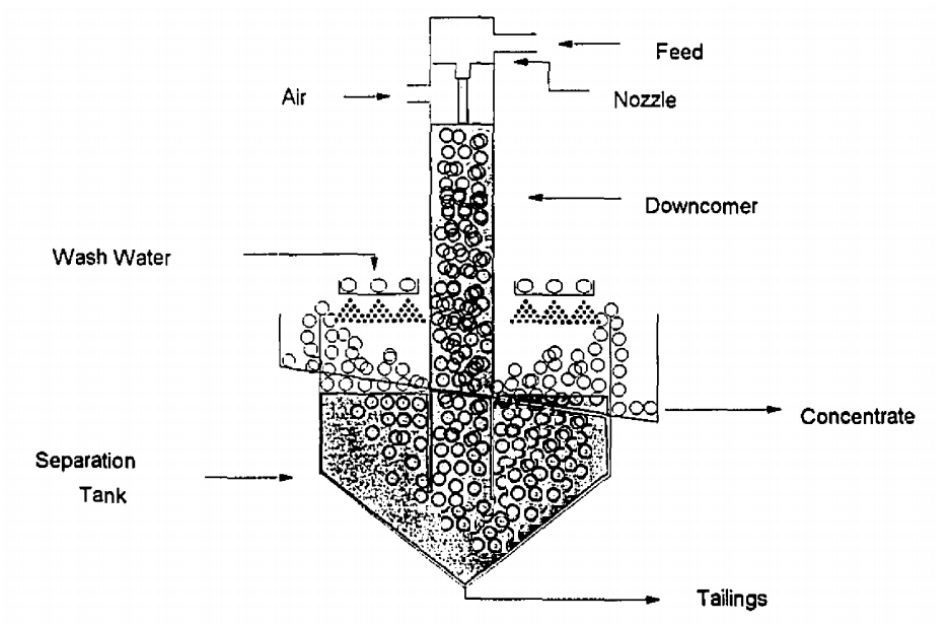

Figure 1: Schematic of Jameson Cell

2.1.1. Industrial Jameson Cell

Even though the patent describes the Jameson Cell as a "flotation column", most bubble-particle interactions take place in the downcomer, the large collection zone of the column no longer being necessary. As Figure 2 shows, the industrial-scale Jameson Cell uses a shallow (separation) tank with multiple downcomers to increase throughput [8]. Bubble diffusers are common installations beneath the downcomer to stabilize the

turbulent bubbly flow exiting the downcomers and to distribute it uniformly across the tank area.

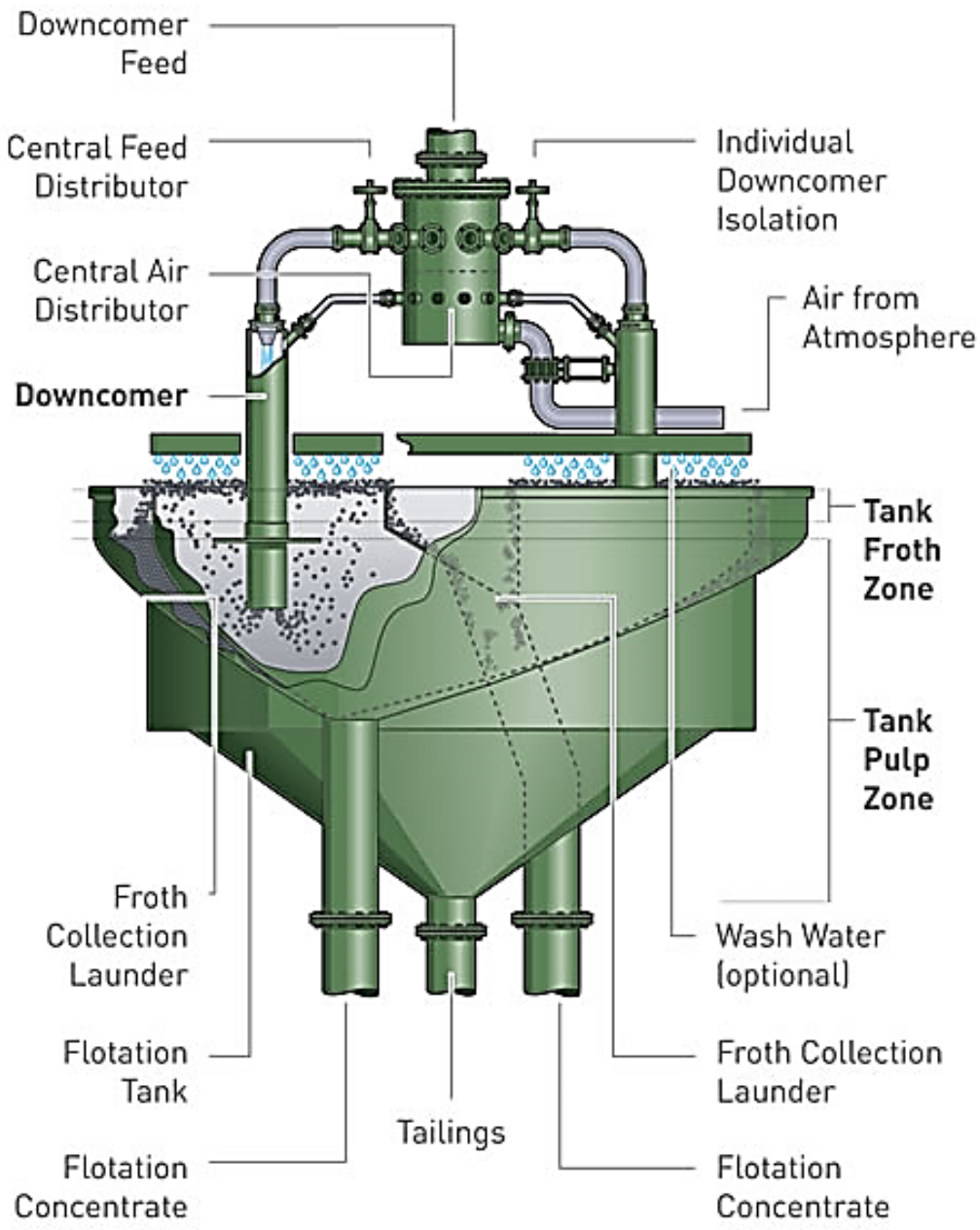

Figure 2: Schematic of industrial Jameson Cell

Wash water is an option depending on the application. Usually, a high concentrate grade favors wash-water addition, and it is used in many coal preparation plants. The wash water distributor typically comprises stainless steel rings with holes with a manual lifting system for inspection and maintenance. Figure 3 shows a wash water system in coal flotation from an Xstrata operation. The wash water system is designed to be applied either above the froth or in the froth. Above froth washing increases froth mobility, at the same time possibly lowering the froth grade; in-froth washing on the other hand results in drier concentrate which may assist downstream filtration [2]. Above froth washing is usually often favored as it facilitates visual inspection.

Figure 3: Wash water system in Jameson Cell for coal flotation[8]

2.1.2. Jameson Cell Development

The first Jameson Cell pilot unit had a throughput of 2 tph; it had a 100mm diameter downcomer with approximately 13mm orifice plate and a test (separation)

tank of 530mm diameter [9]. Subsequently, these dimensions were increased to enable higher throughput. Rectangular tanks were also constructed and test cells started to be incorporated in plants in the early 1990s. Table 1 is an example of increase of downcomer size in the Jameson Cell over the years; along with increase in downcomer size, the number of downcomers per tank has also been increasing.

Table 1: Downcomer size increase over ten years from 1989 to 1999[2]

Year	Downcomer Diameter (mm)	Orifice Diameter (mm)	Flow per Downcomer (m^3/hr)
1989	200	18	14
1990	200	28	30
1993	280	34	50
1997	280	38	60
1999	280	42	75

To date, according to Xstrata literature, typical industrial Jameson Cell tanks can be as large as 6.5m in diameter. Depending on the application, the number of downcomers and downcomer size can be adjusted as well. This gives the Jameson Cell

great flexibility to adapt to many process situations. Table 2 is a reference from Xstrata of different Jameson Cell models and their dimensions.

Table 2: Different Models of Jameson from Xstrata[8]

All-in-one cells (with internal tailing recycle)				
Model	Cell Shape	Flotation tank Dimensions (m)	Number of Downcomers	Fresh Feed Flowrate (m^3/h)
Z1200/1	Circular	1.2	1	50
E1714/2	Rectangular	1.7 x 1.4	2	100
E2514/3	Rectangular	2.5 x 1.4	3	150
E1732/4	Rectangular	1.7 x 3.2	4	200
E2532/6	Rectangular	2.5 x 3.2	6	300
E3432/8	Rectangular	3.4 x 3.2	8	400
E4232/10	Rectangular	4.2 x 3.2	10	500
Circular cells (requiring external tailing recycle)				
B4500/12	Circular	4.5	12	600
B5000/16	Circular	5	16	800
B5400/18	Circular	5.4	18	900
B6000/20	Circular	6	20	1000
B6500/24	Circular	6.5	24	1200

Use of tailings recycle in the Jameson Cell comes from the need to compensate for uneven feed to the unit. The Jameson Cell, to maintain consistent air aspiration rate, has to have constant volumetric feed rate. This recycle feature also helps increase recovery, and protects pumps when fresh feed drops below a certain limit.

The design of the downcomer has gone through significant changes since 1990. As shown in Figure 4, for the first ten years, an orifice plate was used to form the slurry jet. The slurry inlet tube can be readily dis-assembled to allow the orifice plate to be replaced. The most difficult problem was material wear. Different orifice plate

materials were tested including high chromium hardened steel, various ceramics, and high density alumina[6].

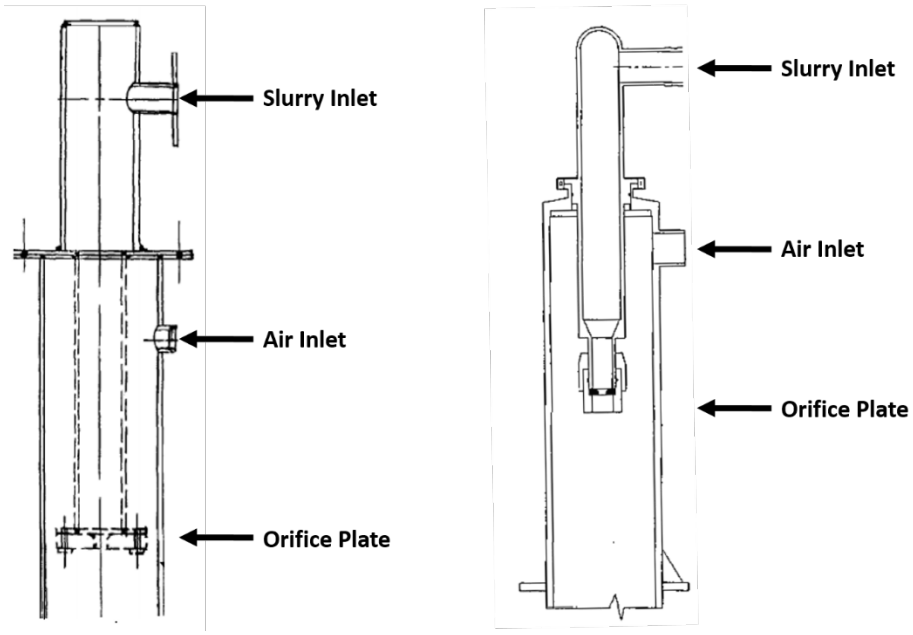

Figure 4: Downcomer developments from 1994-1999

In 1999, the use of a “slurry lens” started to replace orifice plates. As shown in Figure 5, the slurry lens uses a smooth entry angled ceramic to pressurize the slurry flow, thereby reducing the pressure drop associated with the orifice and so lessening material wear. The orifice is cushioned by a polyurethane case so even if the ceramic

is damaged, the polyurethane will retain the orifice shape and remain functional till replaced.

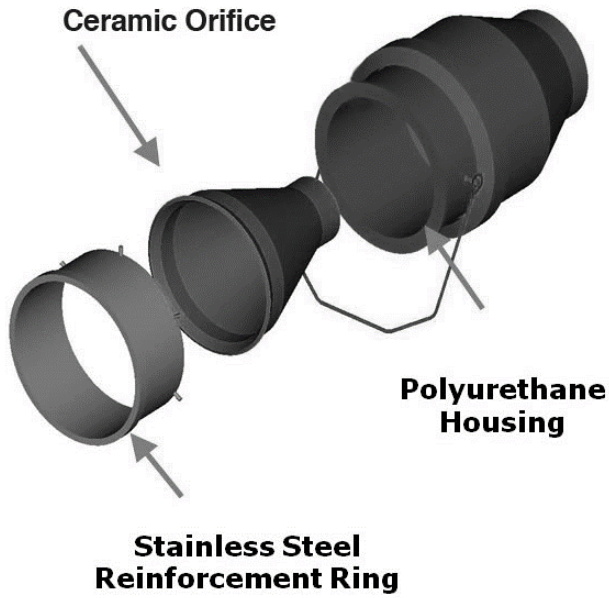

Figure 5: Schematic of slurry lens for Mark III and Mark IV downcomer

In 2000, the new downcomer design, the Mark III, was introduced; it corporates both slurry lens and an AISE (Air Isolating Slurry Eliminating) valve. The AISE valve prevents slurry being drawn into the air valve, acting as "non-return check valve using the concept of a rubber curtain closing against a flat seal" [10]. The AISE valve connects to the downcomer at a 45 degree angle allowing slurry to drain back into the downcomer if any splashes into the air valve. In the Mark III downcomer, both the slurry lens and air valve are separate from the downcomer pipe, this allows convenient dis-assembling for maintenance. The latest downcomer design, the Mark IV, is similar to the Mark III

(as shown in Figure 6) with minor changes to the slurry piping and clamping to enhance flexibility and ease of operation.

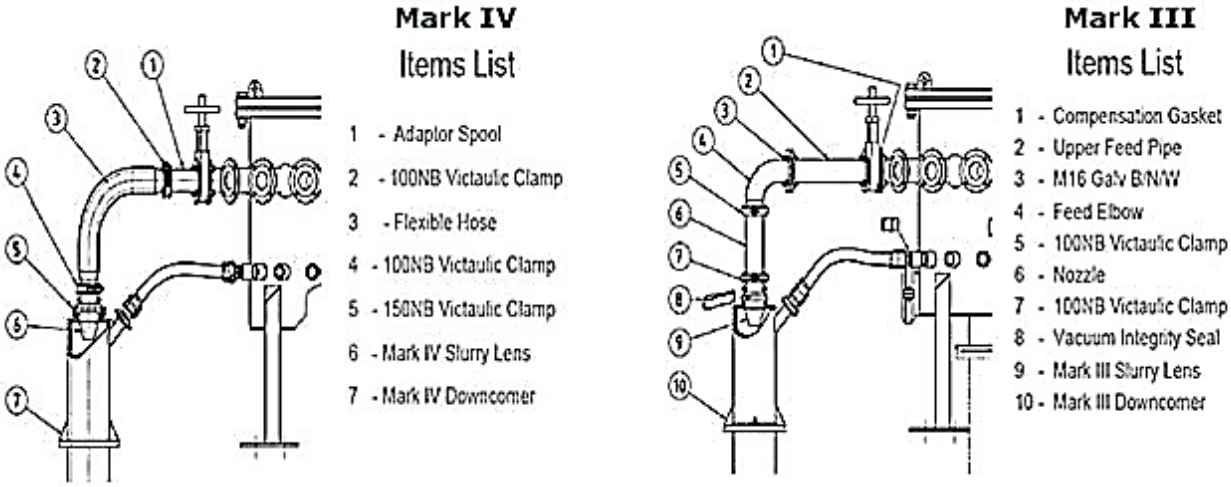

Figure 6: Schematics of Mark III and Mark IV downcomers

2.2. Background of Jameson Cell

2.2.1. Principles of Operation

Downcomer hydrodynamics

The downcomer can also be called a plunging liquid jet reactor (or column). As shown in Figure 7, it consists of three major sections when operating: a free jet, a mixing zone, and a pipe down-flowing zone.

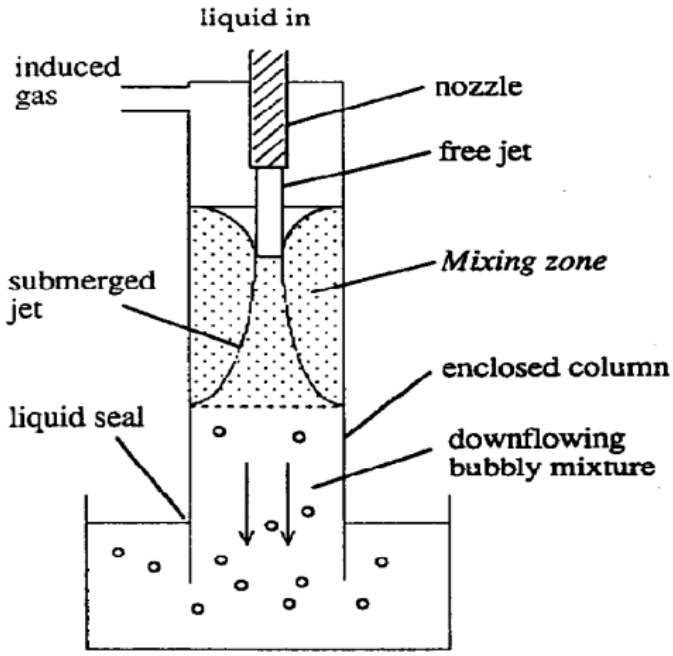

Figure 7: Hydrodynamic zones of a plunging liquid jet reactor[11]

When operating over a certain range of air-to-pulp ratio (APR), a free jet stream is usually visible of a length depending on the APR. The size and velocity of the jet alters as it interact with the surrounding air. Figure 8 illustrates the jet expanding concept: over the length of free jet L_j, part of the air Q_T is entrained by the surface roughness of the jet thereby leading to the apparent jet diameter D_j being higher than the effective diameter D_N. This interpretation was offered by Evans et al. [12], who showed that a free jet with high surface roughness (S) entrains more air than a smooth jet. The "plunging jet" and the "induction trumpet" describe the region where the free jet impacts the fluid surface inside the downcomer. An illustration of a half induction trumpet is shown in Figure 9. The trumpet enters the fluid surface with the air in the

boundary layer and that trapped by its surface roughness. As a result the total amount of air entrained is:

$$QE = Qf + QT \tag{1}$$

that is, the volume of entrained air is the sum of air in the boundary layer and air that is trapped.

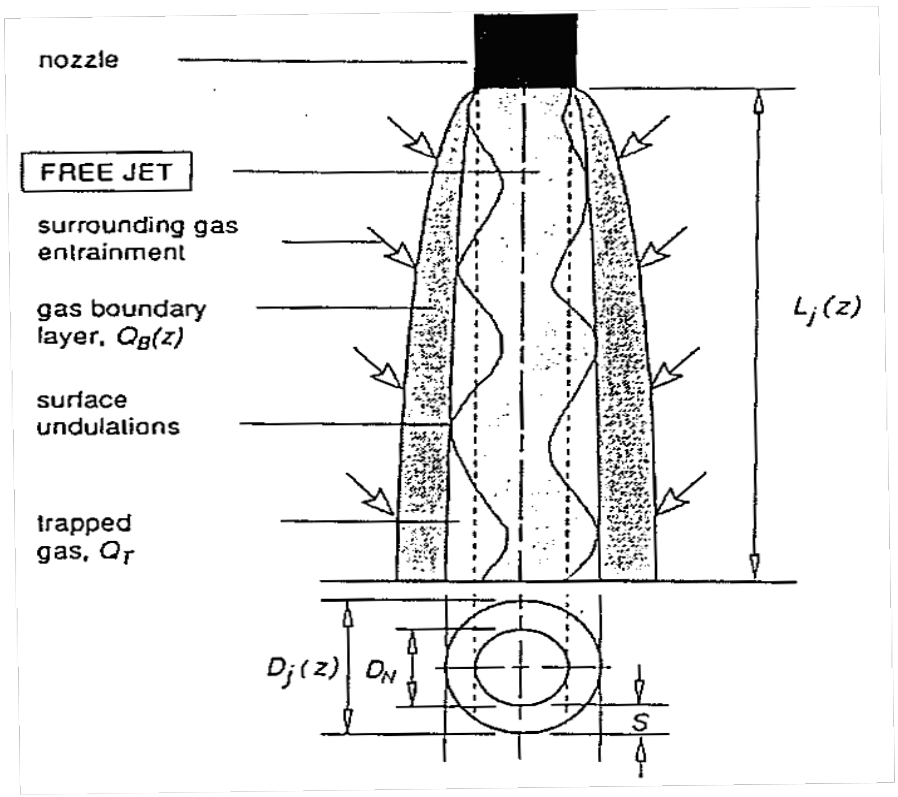

Figure 8: The mechanisms of air transport by a free jet

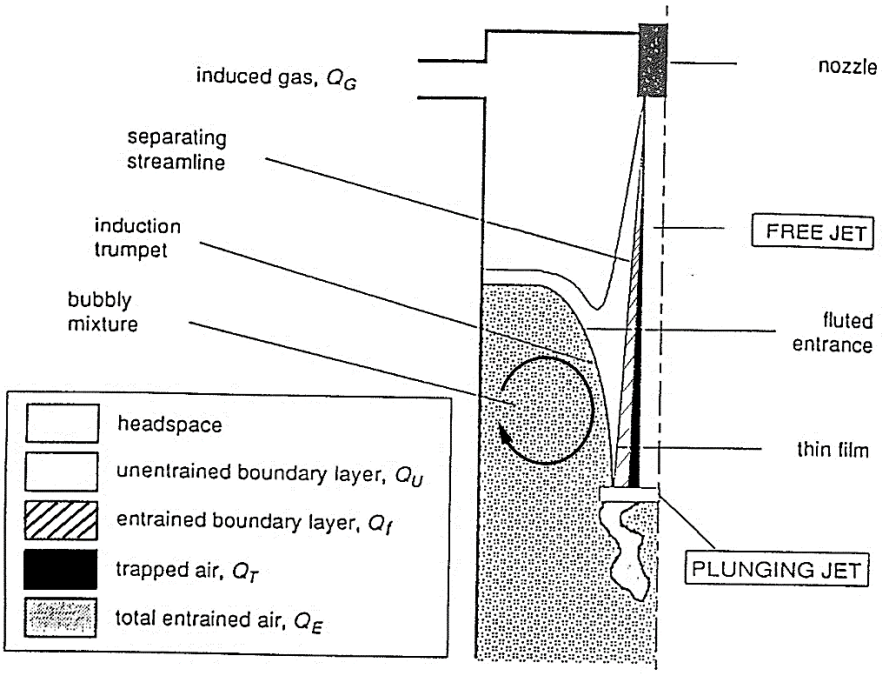

Figure 9: Plunging jet illustration

As the jet collides with the fluid surface, the fluid below the contact point immediately expands and occupies the entire cross-sectional area of the downcomer. Flow recirculates and the turbulence creates many eddies, allowing particles and bubbles to contact and fully mix with each other.

The pipe flow zone is directly under the mixing zone. In this region, the bubbly flow pattern varies depending on air to pulp ratio. At low APR, the bubbles in the flow are small and discrete; if the air flow rate is increased to a certain limit, bubbles coalesce forming air slugs. Therefore, as suggested in Figure 10, bubbly flow is the desired

condition for flotation because it avoids “slugging” and the associated loss in bubble surface area flux and gross disturbance to flow patterns.

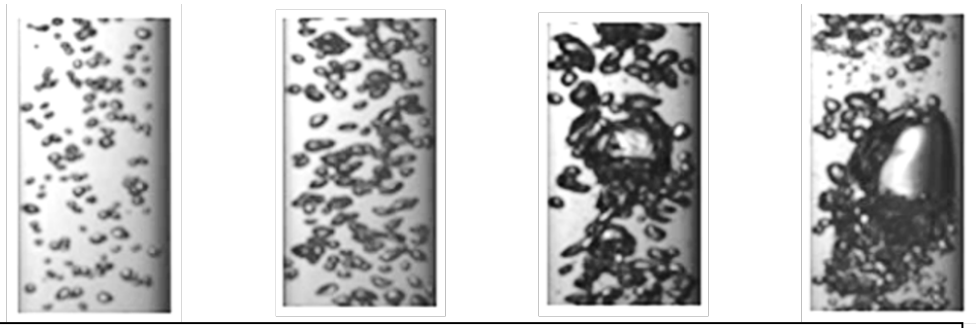

Gas Superficial Velocity (mm/s)	3	15	35	58

Figure 10: Flow regimes in a plunging jet bubble column[13]

Separation Tank

The two important features are that the bottom end of the downcomer is usually below the pulp level in of the tank, and the depth of the froth layer influences the overall recovery. If the froth depth is too high, excessive bubble coalescence will occur leading to the drop-back of collected minerals; on the other hand if the froth layer is too thin, extra gaugue mineral will report to the concentrate due to entrainment. Froth depth is controlled by several operating factors, air flow-rate and feed-rate being the most important. If the air rate (or APR) exceeds a certain limit, the pulp and froth layer lose

the boundary and recovery of gaugue increases[14]. This is usually referred to as "flooding", and means the throughput limit of that Jameson Cell has been exceeded.

2.2.2. Prediction of Bubble Size Generated by Plunging Liquid Jet Reactor

Evans et al. [11] have developed a model to predict the bubble size generated by the plunging liquid jet reactor that could be extended to the Jameson Cell. The theory assumes the energy consumed to generate bubbles comes from the energy dissipated from turbulent flow. In the event of bubble break-up, a bubble is stretched and deformed by the liquid velocity gradient and at the same time preserved by the surface tension on the air-liquid interface. The ratio of such two forces are defined as the Weber number, which can be written as:

$$We = \frac{\rho * (d) * u^2}{\sigma} \tag{2}$$

where u is the average velocity of the jet, d is the bubble diameter, and σ and ρ are surface tension and liquid density, respectively. Therefore the maximum bubble size d_m corresponds to a critical Weber number W_{ec}, because any bubble larger than d_m will breakup into smaller ones.

Assuming the bubble size is small relative to the turbulent macroscale but large compared to the microscale, that is only one turbulent eddy is exerting a force on the bubbles, Hinze (1955) provided a relationship between velocity difference and the

energy dissipation rate per unit volume (represented by E), where constant C is approximately 2 [15]:

$$u^2 = C\frac{(d*E)^{2/3}}{\rho l} \tag{3}$$

Assuming the energy dissipation rate over the mixing zone is uniform, combining equations 2 and 3 will result in a correlation between maximum bubble size (throughout the entire mixing zone) and dissipation energy as shown in the equation below:

$$dm = C * \left(\frac{Wec}{2}\right)^{\frac{3}{5}} * \rho l^{-\frac{1}{5}} * E^{-\frac{1}{5}} \tag{4}$$

Cunningham (1974) provided an analysis of average energy dissipation rate per unit volume in the mixing zone of a plunging jet liquid reactor resolving the energy balance[16]. As a result the specific energy dissipation rate, E, is given by:

$$E = \frac{{u_j}^2}{2} * \left[1 - 2b - b^2(1+\gamma\lambda_1)(1+\lambda_2)^2 + 2b^2(1+\gamma\lambda_1)(1+\lambda_2) - \frac{2\gamma\lambda_1 b^2}{1-b} + \gamma{\lambda_1}^3\frac{b^2}{(1-b)^2}\right] - \frac{\lambda_1 P_1}{\rho}\ln\frac{P_2}{P_1} \tag{5}$$

where ρ is the liquid density, u_j is the jet velocity, λ is the gas/liquid volumetric flow ratio, γ is the gas/liquid density ratio, b is the jet/column area ratio, P is the absolute pressure where P_1 is the inlet pressure and P_2 is the outlet pressure of a mixing zone area. Equation 5 can be simplified by assuming the gas/liquid density ratio equals zero (γ=0), and the pressure difference across the mixing zone is zero (P1=P2). Taking the energy dissipation rate per unit volume times the mass flowrate of the jet per unit

volume and dividing by the mixing zone total volume, the final energy dissipation equation is as following:

$$E = \frac{\rho * {u_j}^3}{2*L} * [b - 2b^2 - b^3(1+\lambda_1)^2 + 2b^3(1+\lambda_1)] \quad (6)$$

where L represents the mixing zone length. Equation 6 can be used with equation 4 to predict the maximum bubble size generated in a plunging liquid reactor[11].

According to Evans et al. [11]there have been several attempts to determine the critical Weber number, however, they differ in setup and flow conditions. A recent reference shows that critical Weber number is a function of the Reynolds number and ranges from 0.95-2.76 for a uniaxial extensional Newtonian flow[17]. Although the critical Weber number is influenced by several factors, one could estimate the critical number for a given setup by measuring the bubble size generated. This requires knowing the mixing zone length (L), which is another challenge, Evans et al. [11] installed pressure taps along a downcomer, and for different operating conditions (different APR) similar results of mixing zone length were obtained. Figure 11 shows the predicted bubble size are within 20% errors of the measured, proving the reliability

the bubble size prediction method [11]. Bubble size as small as 200µm were reported in later work from the same team.

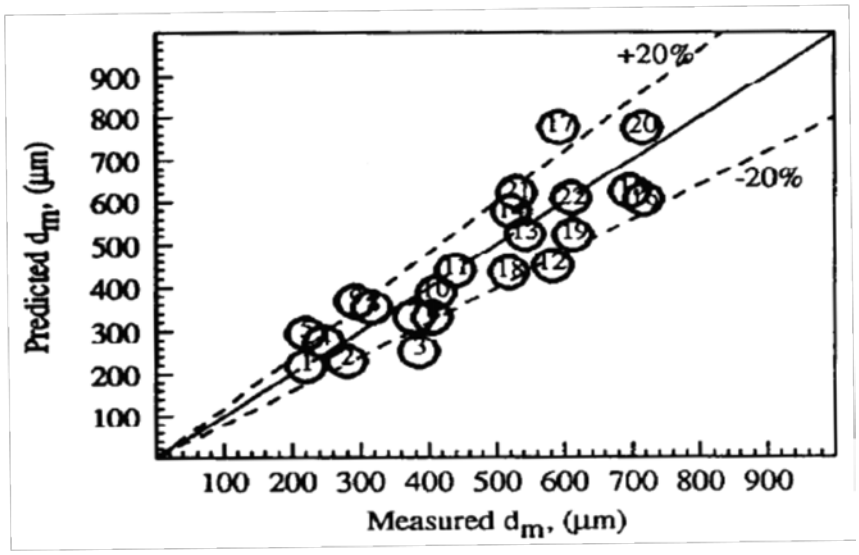

Figure 11: Comparison between predicted and measured maximum bubble diameter

2.3. Operating Conditions and Controlled Variables in Jameson Cell

2.3.1. Primary Variables

The factors that affect the Jameson Cell can be divided between those that relate to cell design, and those that relate to operation. As shown in Figure 12 and Figure 13, the cell design (geometry) of a Jameson Cell covers a range of possibilities: orifice plate size and shape, or the slurry lens size; downcomer diameter, length, number and positioning in the separation tank; tank shape, diameter, and depth. Of those related to operation, the most basic would be those that control recovery, primarily air and slurry flowrate, and possibly accessories such as wash water flowrate. Other factors, the usual physical ones, mineral properties, percent solids, and particle size distribution, remain crucial, as do the chemical variables, that is, type and dosage of frother, collector, and

regulators. In this thesis, the influence of some of these design and operational variables will be investigated.

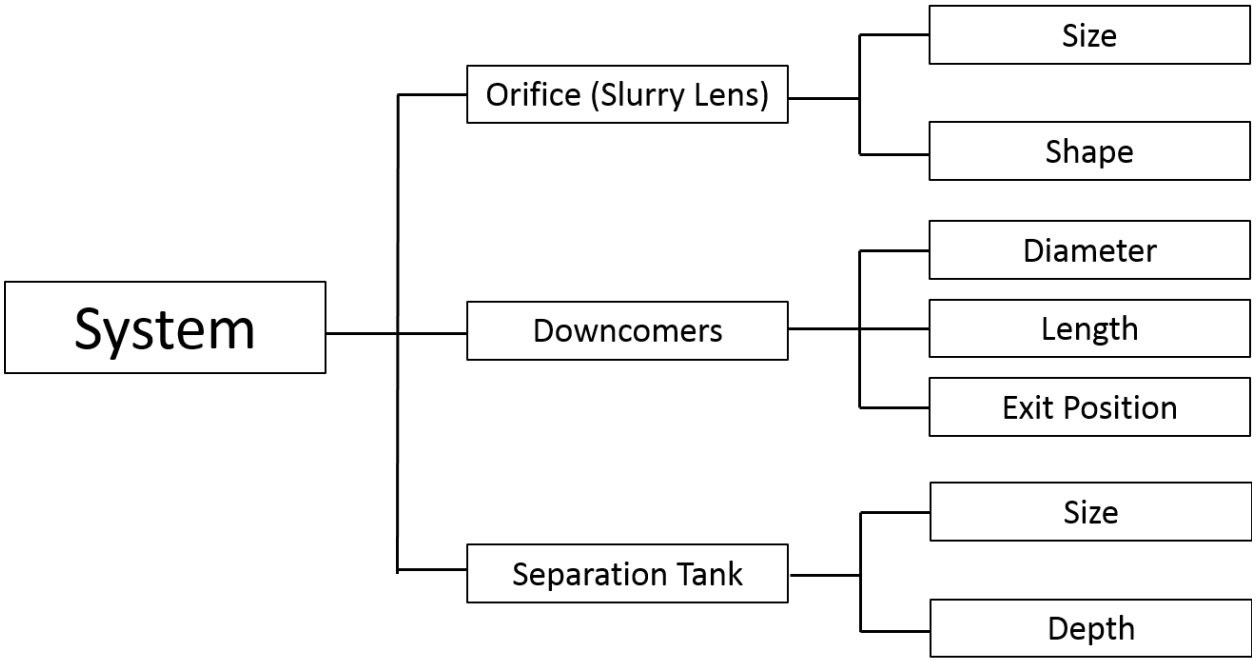

Figure 12: Variables in Jameson Cell operation

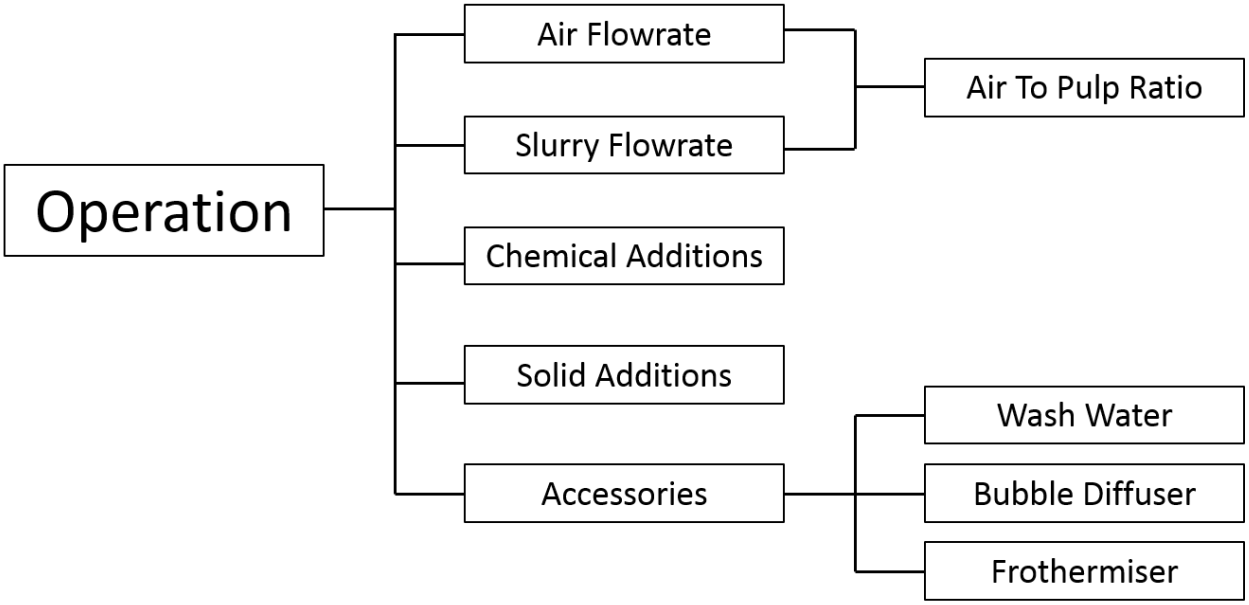

Figure 13: Variables of Jameson Cell operation

2.3.2. Secondary Variables

The secondary factors include: Downcomer jet conditions (or sometimes referred to as bubbly mixture height in the downcomer), residence time (in the downcomer), air-to-pulp ratio, froth depth, superficial gas velocity, gas holdup (void fraction), bubble size, wash water rate and solids carrying capacity.

Downcomer Jet Conditions and Residence Time

The combined length of the mixing zone and pipeflow zone is limited by and approximately equal to the total length of downcomer minus the free jet length. The air-to-pulp ratio (APR) will have an effect on the hydrostatic pressure inside the downcomer and thus it determines the length of free jet and mixing zone. An increase in APR lengthens the free jet and lowers the vacuum pressure which compromise the mixing zone length as illustrated in Figure 14. Reduced mixing zone length does not significantly increase bubble size but does reduce residence time, giving particles and bubbles less time to contact. Results of experiments by Tasdemir et al.[18] on recovery of quartz from Jameson Cell are shown in Figure 15. From these findings, higher jet length results in shorter mixing zone and therefore lower recovery of coarse quartz particles. This follows as the longer jet means a shorter bubbly mixture height in the

downcomer giving less opportunity for the high settling rate coarse particles to attach to bubbles.

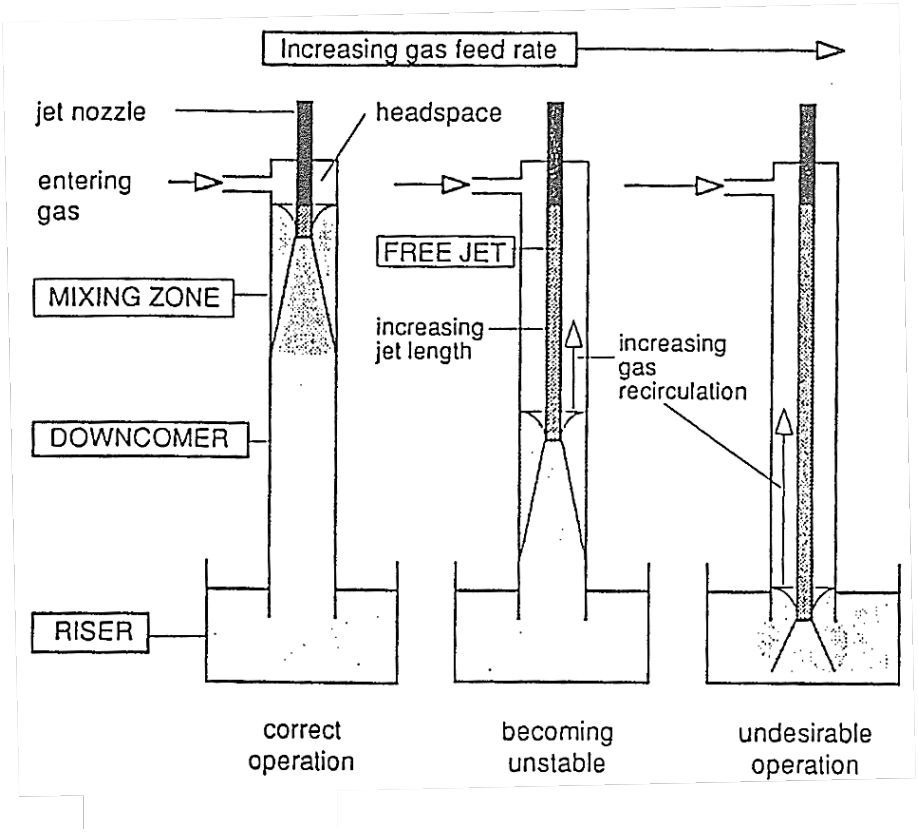

Figure 14: Variation of free jet length [3]

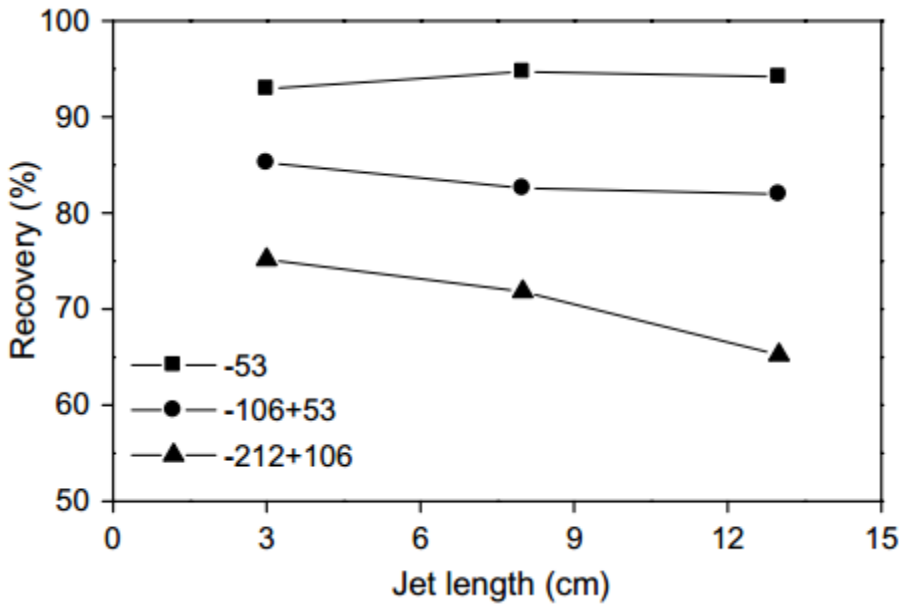

Figure 15: The effect of jet length on recovery in the downcomer[19]

Froth Depth

Shallow froth depths (less than 200mm), while allowing more particles to report to the concentrate, do so at the cost of extra entrainment of fine gangue particles, thus decreasing the grade. On the other hand, while large froth depth means more particles drop back into the pulp, it significantly reduces water recovery and entrainment, which enhances grade at the expense of recovery. Building deep froths is aided by wash water which also affects water content in the froth (froth "dryness") [20]. Jameson and

Manlapig [21] observed decreased recovery with increased froth depth, as shown in Figure 16.

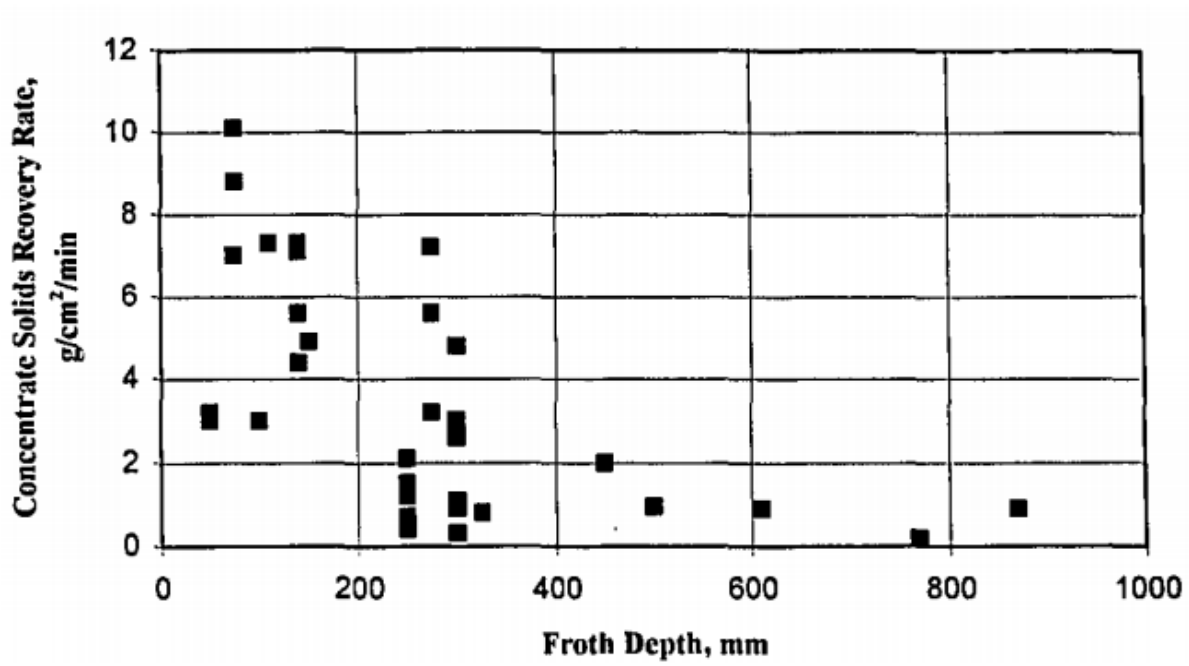

Figure 16: Concentrate solids production rate vs. froth depth[21]

Superficial Gas Velocity

The superficial gas velocity, commonly symbolized as J_g, is calculated from the air flowrate divided by the cell cross-sectional area. Typically, the J_g in mechanical and column flotation machines is around 0.5 to 4 cm/s [1]. In general, cleaning application apply low J_g (typically from 0.4 to 0.8 cm/s) because feed is high grade and low J_g creates stable fully loaded froth. This allows deep froths to build which helps eliminate entrainment raising the grade of concentrate. On the other hand, roughing and scavenging apply higher J_g.

Defining the J_g in a Jameson Cell requires a little thought as it could be defined either on the basis of the downcomer or the separation tank. In the downcomer J_g can

be over 20cm/s. Such high J_g creates high gas holdup and so high bubble surface area flux. In contrast the J_g in the tank is often similar to the J_g quoted above for mechanical cells and columns. The J_g also controls bubble size; high J_g giving larger bubbles [22].

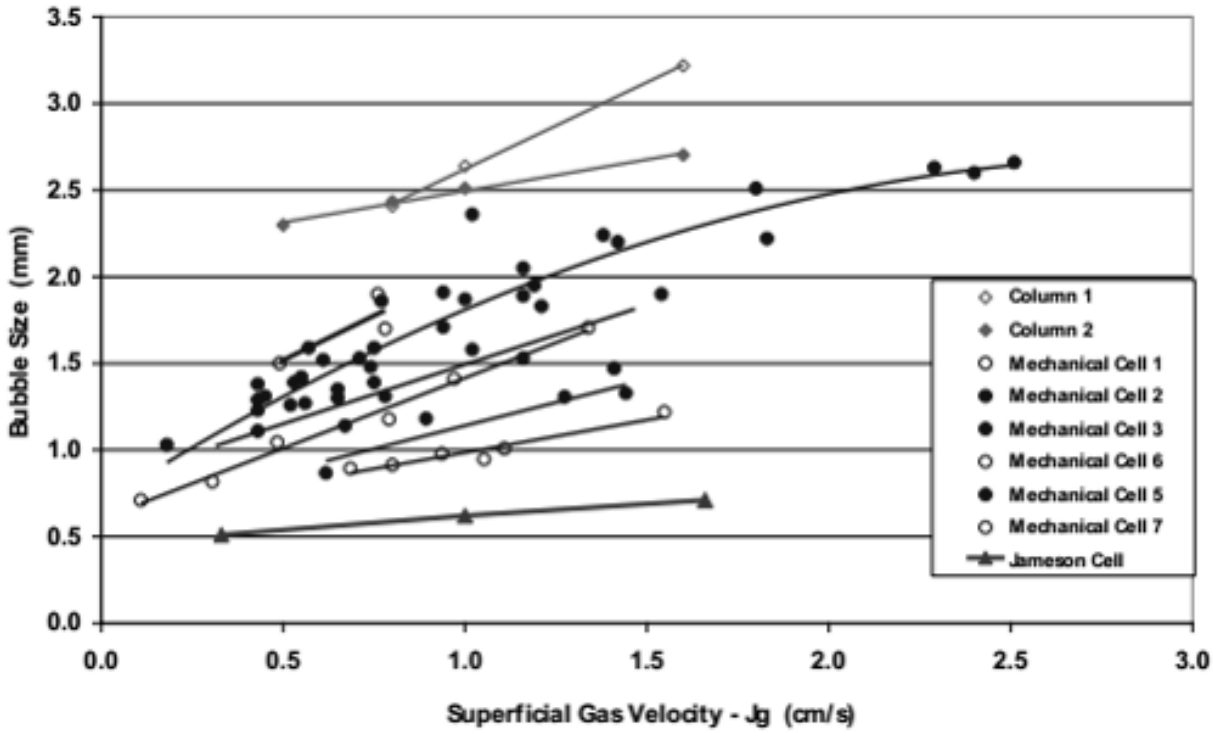

Figure 17: Bubble size as a function of Jg for different flotation machines[22]

Gas Holdup (Fluid Void Fraction)

Gas Holdup or void fraction is calculated as follows:

$$\epsilon = \frac{Vg}{Vg+Vl} \tag{7}$$

where Vg and V_l are volumes of gas and liquid, respectively: that is, gas holdup is the volume fraction of air inside the slurry. There are two common ways of automatically measuring gas holdup, through conductivity, and through pressure difference. Both will be introduced later. Gas holdup represents how much air resides in the slurry and is a

combined result of air flowrate and bubble size. In mechanical and column cells, small bubbles create high gas holdup because they rise more slowly than large bubbles; that is they have higher retention time in the slurry. In such machines gas holdup reaches about 15%, above this air slugs form and the flow is disturbed, the cell having the appearance of “boiling”. In the Jameson Cell downcomer, much higher gas holdups are observed, that also increases as bubble size is reduced (e.g. by adding frother) reaching up to ca. 60% [23]. It has been shown that jet velocity, downcomer size and orifice size affect gas holdup [18]. Figure 18 shows gas holdup responds positively to jet velocity for different setups: A, fixed downcomer and orifice size but different jet length; B, fixed downcomer and jet length but different orifice diameter; C, fixed orifice and jet length but different downcomer diameter [18]. The Jameson Cell is noteworthy for its high gas holdup in the downcomer typically around 50%; many maintain that this encourages particle collection yet the mechanism of particle collection in the downcomer has not been fully determined. Considering the relationship between jet velocity and gas hold up in the downcomer, the following are observed: as the free jet length increases, the gas holdup increases; smaller jet diameter (smaller orifice

diameter) results in higher gas hold up; and increasing downcomer diameter increases the gas holdup.

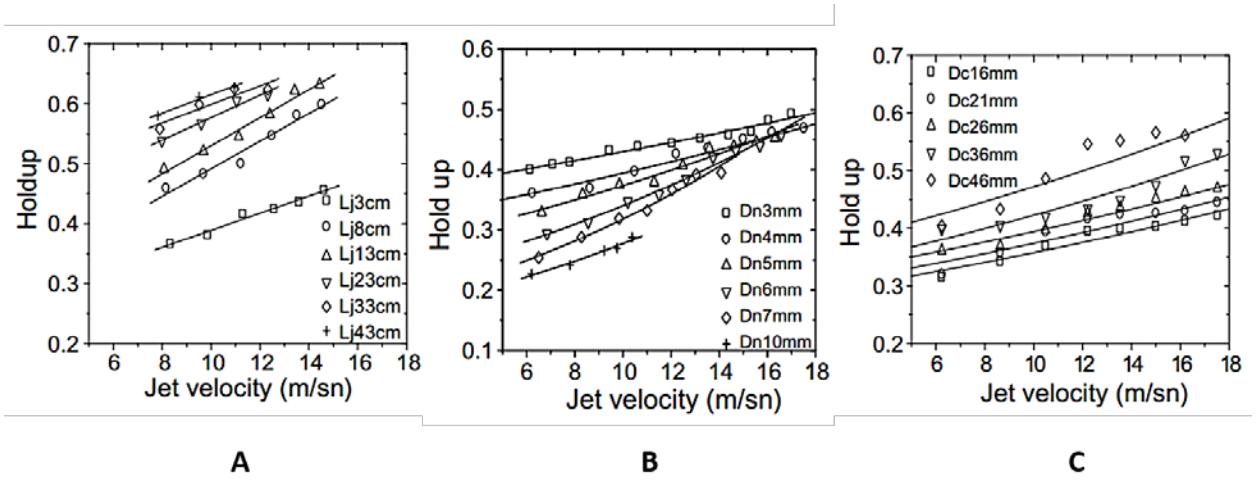

Figure 18: Gas holdup in Jameson Cell downcomer response to jet velocity under different setups

Bubble Size

Bubbles are the carriers of the collected particles, and bubble sizes is the result of all the primary factors discussed above. As Evans et al. [11] and Jameson et al. [24] have demonstrated the Jameson Cell is capable of generating bubbles as small as 300 µm. When compared to other flotation machines, the Jameson Cell generates comparatively small bubbles, as indicated in Figure 17 and noted in the literature [25]. Small bubbles yield high gas holdup and high bubble surface area flux in the pulp zone,

and also promote froth stability [26]. In this thesis, how hydrodynamic conditions in the Jameson Cell control the bubble size will be investigated.

2.3.3. Jameson Cell Particle Collection Mechanisms

In regards particle collection in the downcomer, different hypotheses have been proposed and can be classified into four types [27]:

- Thin-film migration collection
- Instantaneous collection
- Residence time dependent collection
- Mixing zone extended to tank zone collection

The thin-film migration theory is based on the fact that the gas holdup in the downcomer (both mixing zone and pipe flow zone) is high meaning the distance between bubbles ("films") is short so that the particles distributed in the films do not have far to reach a bubble surface. [24]. Collection is, therefore, less influenced by the residence time and the probability of contact between particles and bubble is no longer a determining factor. This theory suggests that keeping a high vacuum in the downcomer is not important to particle collection in a Jameson Cell.

The instantaneous collection mechanism emphasizes that the there is no minimum vacuum nor residence time requirement in the downcomer [27].

The residence time dependent collection mechanism adapts the "kinetic" theories accepted for mechanical cells and flotation columns. These kinetic theories involve collision, bubble-particle attachment, and detachment mechanisms. This suggests high

vacuum is favored to increase the bubbly mixture height and residence time in the downcomer.

Another theory raises doubts as to whether the particle collection is wholly within the downcomer region. The argument is that the strong turbulence within the downcomer while it does promote collision between particles and bubbles, also encourages detachment of particles. Part of the particle collection process may extend into the separation tank where the bubbly swam is more typical of mechanical machines and columns. While particle collection is not involved in the present work the thesis does cover effects on the mixing zone length, which may be related to particle collection.

Chapter 3: Experimental Apparatus

3.1. Jameson Cell Developed at McGill University

The laboratory Jameson Cell constructed at McGill University is a closed circuit setup, comprising a conditioning tank, separation tank, downcomer and orifice plate, bubble viewer, various other sensors, and a data collection system (Figure 19). The conditioning tank holds 200 liters of solution agitated with a magnetic mixer. The separation tank is 2.5 m long (L=2.5m), with base diameter (D) 25cm, and the total volume approximately 125 liters. The separation tank has an overflow launder and the overflow drains back to the conditioning tank or can be directed for collection. The underflow is connected to the level control tube, which can be adjusted up and down so that the level (froth depth) in the separation tank can be changed manually regardless of other operating conditions. All the test work uses water only, that is, no particles as the lab is not designed for handling large volumes of slurry.

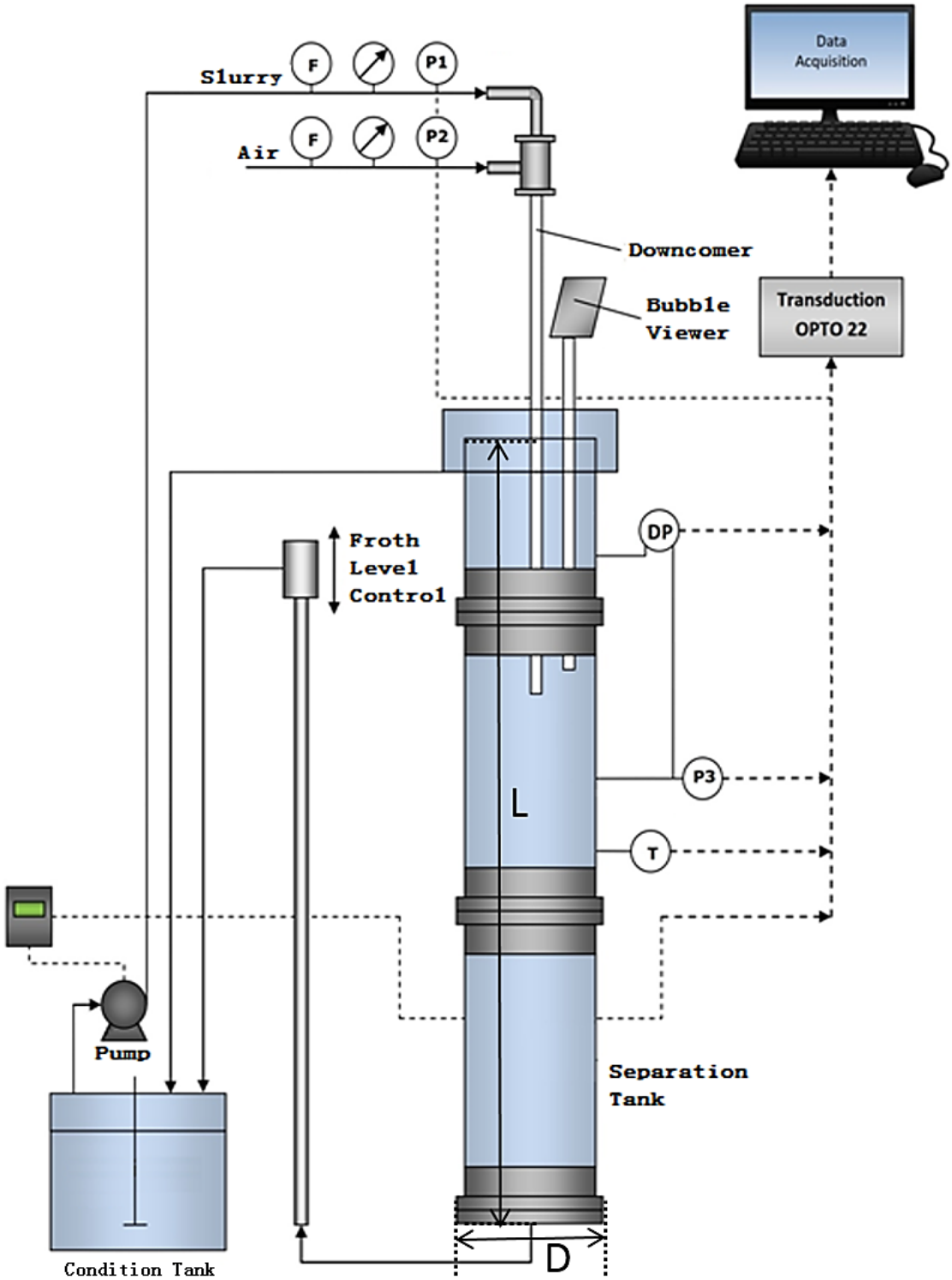

Figure 19: Schematic of the laboratory Jameson Cell

The downcomer design is shown in Figure 20. Unlike current industrial design, the original orifice plate design, with its opening parallel to the liquid flow, is used to pressurize the jet. The diameter orifice plate, D_o, is a test variable. The downcomer has a diameter of D_d and length of L_d; its outlet is always set to approximately 46cm below the liquid surface and both D_d and L_d are variables in the experiment design.

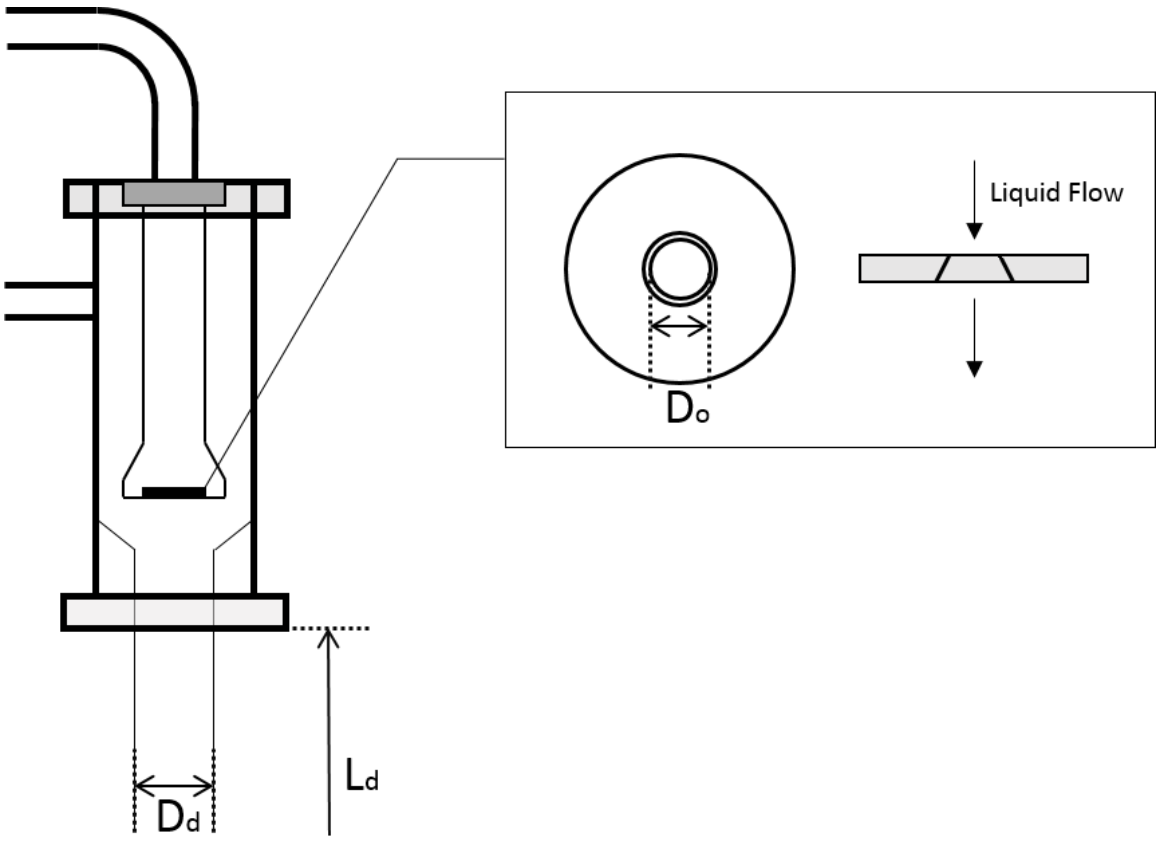

Figure 20: Jameson Cell apparatus at McGill – downcomer illustration

The bubbles are sized using with the McGill Bubble Size Analyzer (bubble viewer). The sampling point is in separation tank approximately 10cm above the downcomer outlet

where the static pressure is monitored for bubble size correction. The technique of bubble size determination is discussed in section 4.2 and bubble size correction in section 4.3.

Various sensors are used to monitor aspects of the experiment, as shown in Figure 21, (the symbols are related to the Jameson Cell schematic, Figure 19). Pressure sensors, gauges, and flowmeters are installed on both the liquid and air flow streams. On the separation tank there is a differential pressure sensor. Pressure and temperature sensors are monitored in the Jameson Cell, and the atmospheric pressure sensor is deployed in the room.

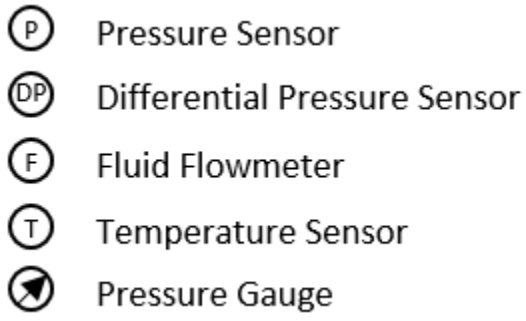

Figure 21: Sensor Deployments

3.2. Data Acquisition Techniques

3.2.1. Major Sensors Deployed on Jameson Cell at McGill

Pressure Transmitters

These are double-wire NOSHOK 600 series pressure transmitters, as shown in Figure 22. They are resistant to vibration and shock and calibrated manually at least once a year. Pressure transmitters are installed on both the liquid and air feed pipe lines ahead of the downcomer. A pressure transmitter is installed at a fixed point on the

separation tank to monitor the absolute static pressure at that location, as shown in Figure 19. The pressure sensor measurement ranges up to 30psi, which is sufficient for the current installation.

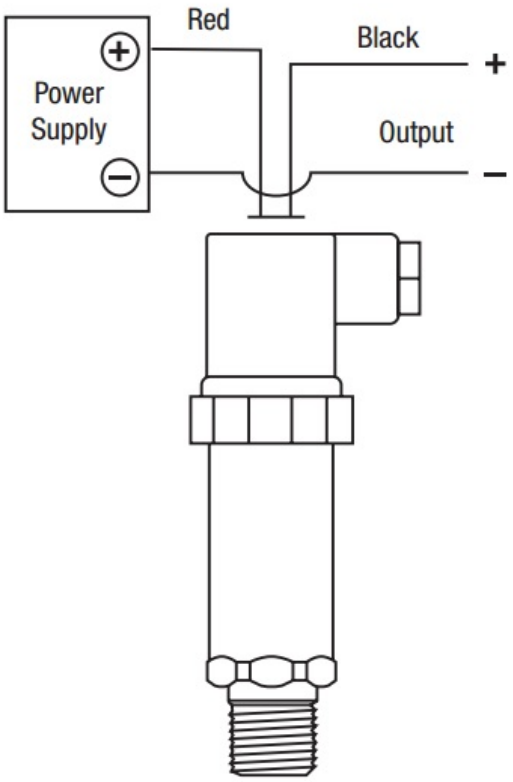

Figure 22: NOSHOK pressure transmitters

Differential Pressure Transmitter

This is a 266 series differential pressure transmitter from ABB Ltd. It measures the difference of static pressure in two (plastic) tubes filled with water tapped at two

locations on the separation tank. The distance between tapping points is 52cm. The differential pressure is used to determine the gas holdup value within the 52cm section.

Liquid Flowmeter

The slurry flowmeter (50XM1000N Magnetic Flowmeter Converter manufactured by Bailey Fischer& Porter Ltd) is installed as shown in Figure 23. It measures slurry flowrate and transmits the signal to a data recorder. The measurement range is 0 to 50 L/min, although the maximum flowrate is limited by the pump capacity and the downcomer orifice size, as will be discussed later.

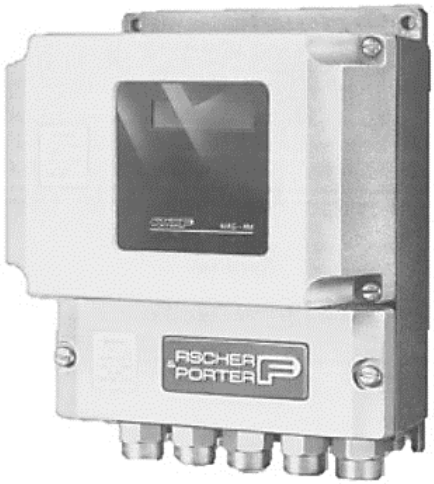

Figure 23: Magnetic flowmeter

Air Flowmeter

The air flow measurement comprises both non-electronic and electronic devices to check accuracy and give flexibility. The (non-electronic) rotameter is simple to install

and read but less accurate than the electronic device, and was used when performing quick system checks. Both controlled and non-controlled air flowmeters were used on different lines. Mostly, MKS mass flow controllers were used with flowrates ranging up to 50 L/min. This type of controller can receive signals to provide a flowrate set point and then measure the true flowrate sending this signal value back to the control software. Since the air is self-aspirated (due to the vacuum generated by the jet), it is not, in one sense, controlled but is measured. These digital mass flowmeters provided the high accuracy needed for this research.

3.2.2. McGill Bubble Viewer

The bubble viewer used at McGill University is essentially a sealed visualization chamber, as shown in Figure 24. The chamber is constructed with two glass windows, one in the front and one at the rear. Before collecting bubbles, the chamber is filled with liquid (usually frother-containing water) and sealed. The sampling tube allows bubbles to rise into the chamber and images of the bubbles are taken. The slight incline of the

chamber (15 deg. to vertical) allows bubbles to spread out and slide along the underside of the glass window to provide an unambiguous focal plane.

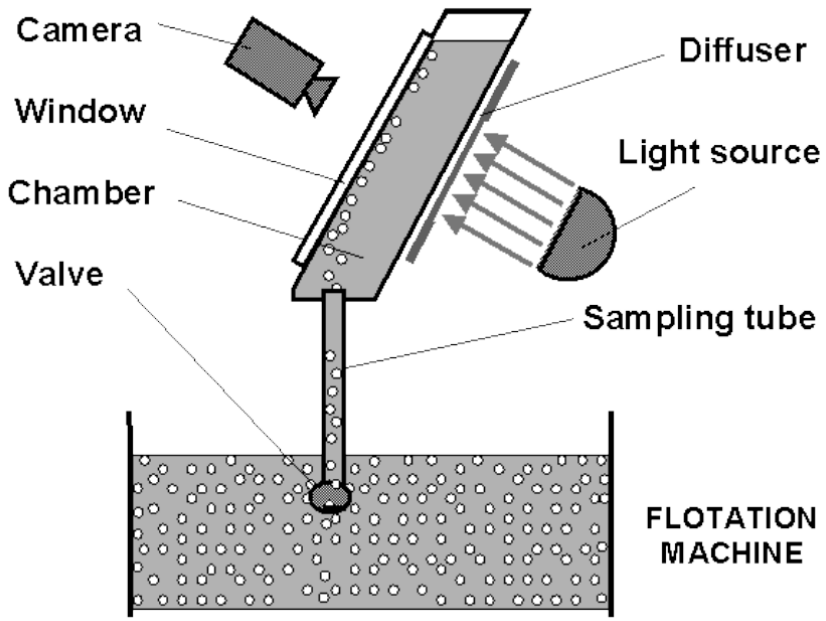

Figure 24: Schematic illustration of McGill Bubble Viewer

Chapter 4. Experimental Procedures and Sample Calculations

4.1. General Procedure

The experiments were conducted using a two-phase water-air, a two-phase system with a variation of frother dosage to control bubble size. The general steps in the experiment are presented below:

1. All accessories to be used were checked to make sure they were functioning properly prior to any experiment, including sensors and cameras.
2. Frother dosage was calculated and measured using an analytical lab scale.
3. Solution temperature of ca. 20℃ was targeted. During winter, the tank water was prepared the day before the experiment to allow it warm to room temperature.
4. Frother (DF250) was added into the conditioning tank, followed by a minimum of 5 minute stirring by a magnetic mixer.
5. Solution pump was turned on and circulation started between the Jameson Cell and conditioning tank; upon reaching steady state level in the conditioning tank, that is, when overflow equals inflow, air and solution flowrates were adjusted according to the experiment design.
6. If bubble size data were to be collected, samples to the bubble viewer were taken after circulation was stable.
7. The start and end time of the experiment was recorded. A minimum of 5 minutes of stable operation was established as minimum prior to taking measurements for each set of conditions; typical duration of each experiment (i.e., testing one set of conditions) was ca. 10 minutes.

8. When the experiment was finished, the pump was turned off and the tanks were drained. The separation tank and conditioning tank were thoroughly cleaned, especially if a different frother dosage was to be tested.

9. Sensor signals were collected continuously.

4.2. Bubble Sizing Technique

4.2.1. Bubble Size Data Management

Typically over 20,000 individual bubbles were imaged to yield various mean values. The most straightforward is the arithmetic mean:

$$\mathbf{nd_{10} = \Sigma d_i\ n = \Sigma n_i}$$

$$\mathbf{d_{10} = \frac{\Sigma d_i}{n}}$$

where d_{10} represents the average diameter, the subscript 10 represents the sum of one exponential (diameter) over the sum of bubble counts. On this basis, an average (mean) diameter could be represented by many possibilities, such d_{10}, d_{21} and d_{32}. Taking d_{32} (also called the Sauter mean diameter) as an example, the calculation is:

$$\mathbf{n} * \frac{\boldsymbol{\pi}}{\mathbf{6}} * \boldsymbol{d_{32}^3} = \mathbf{\Sigma}(\frac{\boldsymbol{\pi}}{\mathbf{6}} * \boldsymbol{d_i^3})$$

$$\mathbf{d_{32} = \frac{\Sigma d_i^3}{\Sigma d_i^2}}$$

The resulting d_{32} is one-dimensional quantity representing the average diameter calculated from the sum of the volume of all bubbles divided by the sum of surface area

of all bubbles. Given that particle collection is driven by the surface area of bubbles, the d_{32} is the most common mean used in flotation studies.

Mathematically, in the range d_{10} to d_{32} all the possible diameter calculations (e.g. d_{20}, d_{30} and d_{31}) lie within the numerical range of d_{10} and d_{32} (calculations beyond the 4th exponential presents no physical meaning). As an example, the following table is a sample calculation result of 5 bubbles with size 1,2,3,4 and 5 to demonstrate the range in calculated mean values:

d_{10}	**d from d_{20}**	**d_{21}**	**d from d_{30}**	**d from d_{31}**	**d_{32}**
3.000	3.317	3.667	3.557	3.873	4.091

Therefore, in presenting the bubble size of a swarm, the d_{10} is considered the minimum and d_{32} is the maximum, and, as noted d_{32} is the most often used in flotation system studies.

A swarm of fine bubbles, and Figure 25 gives an example, can easily be achieved with the use of frother or salt.

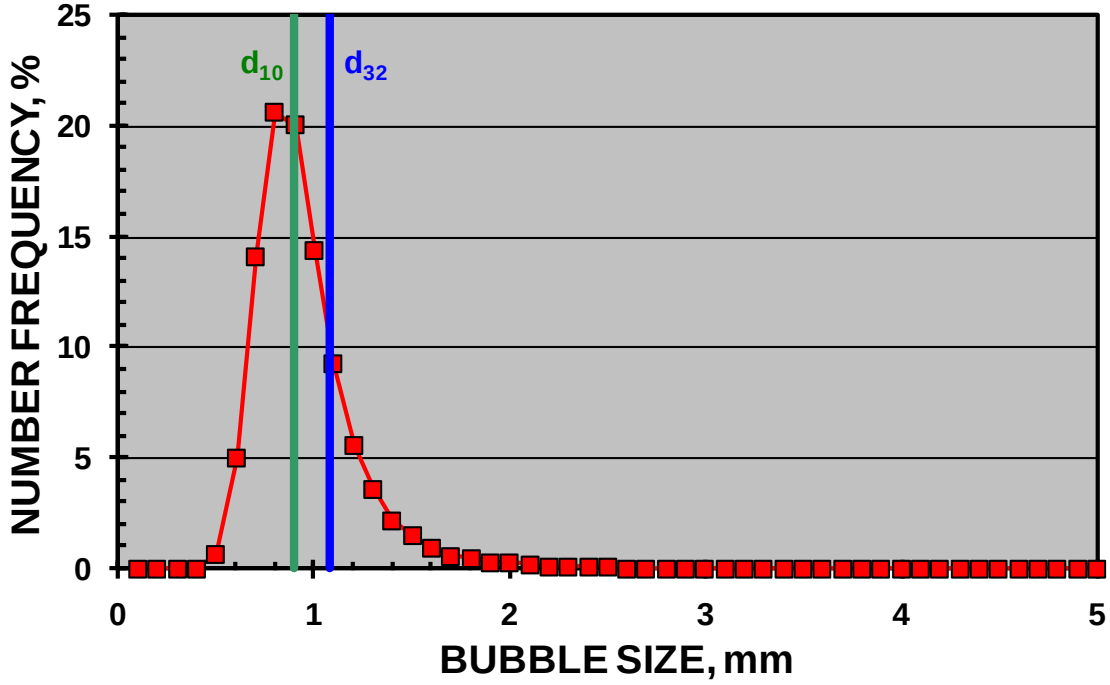

Figure 25: A sample of bubble size frequency of a bubble collection

4.2.2. Bubble Sizing Method

A typical experiment yielded over 200 images. Each picture may contain several to hundreds of bubbles. An example is used to illustrate the procedure. Figure 26 is a sample of bubbles taken with the McGill Bubble Viewer for a solution of 5ppm DF250 at 15 L/min air and solution flowrate. Bubbles are spherical and have good contrast against the background. There are some bubbles slightly out of focus and some bubbles

are clustered. The scale of the sample picture has been measured as 203.45 pixels per mm.

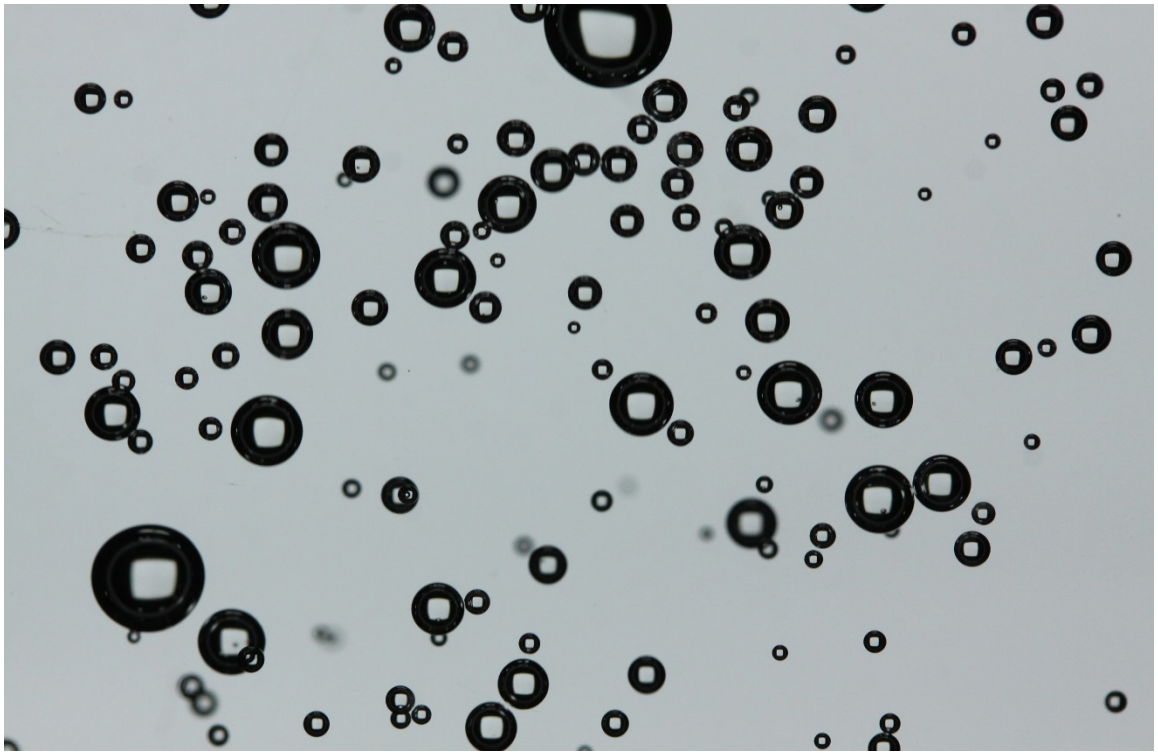

Figure 26: Sample bubble picture, original

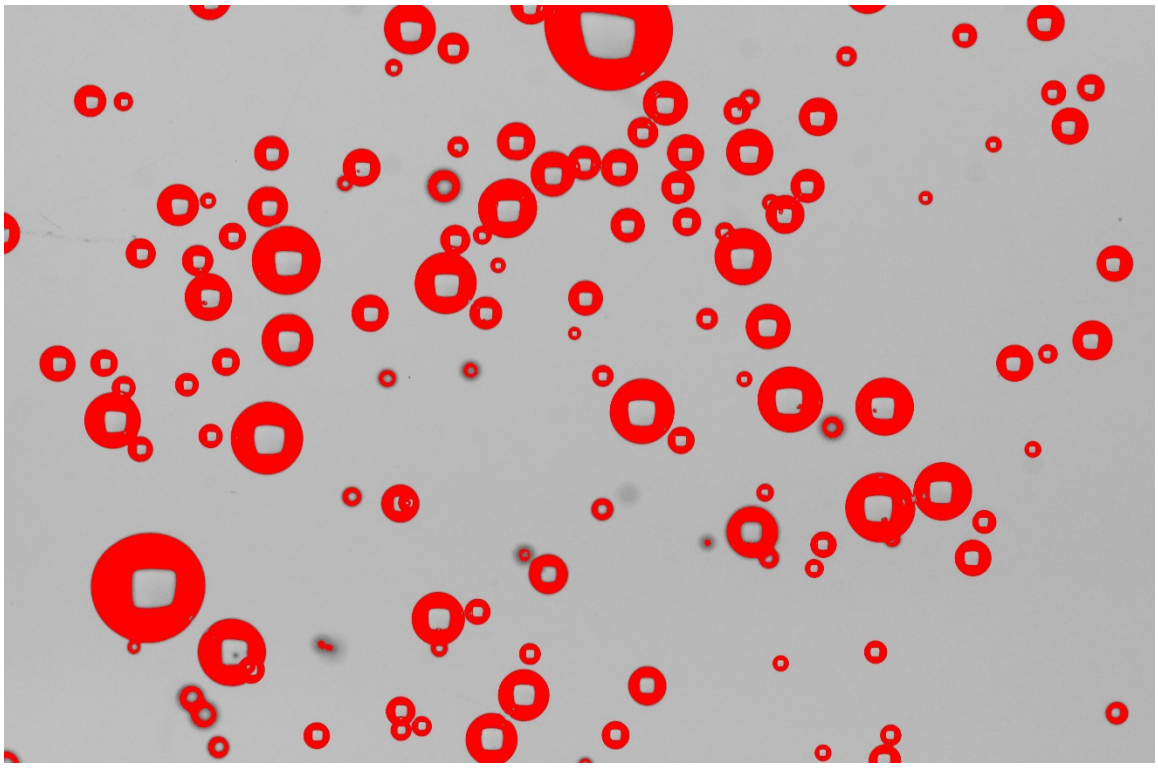

Figure 27: Sample bubble picture, contrast threshold applied

To enable the image processing software to detect the target objects (bubbles), a contrast threshold is applied. This step was usually done automatically. In the event the camera setting was not ideal, that is, bubbles were not as clear as they should be, or the contrast of bubbles and background was not adequate, manual threshold adjustment helped enhance the result. Given the required circularity and minimum and maximum

bubble size expected, the software will determine the spheres in the picture that fit the criteria as shown in Figure 28.

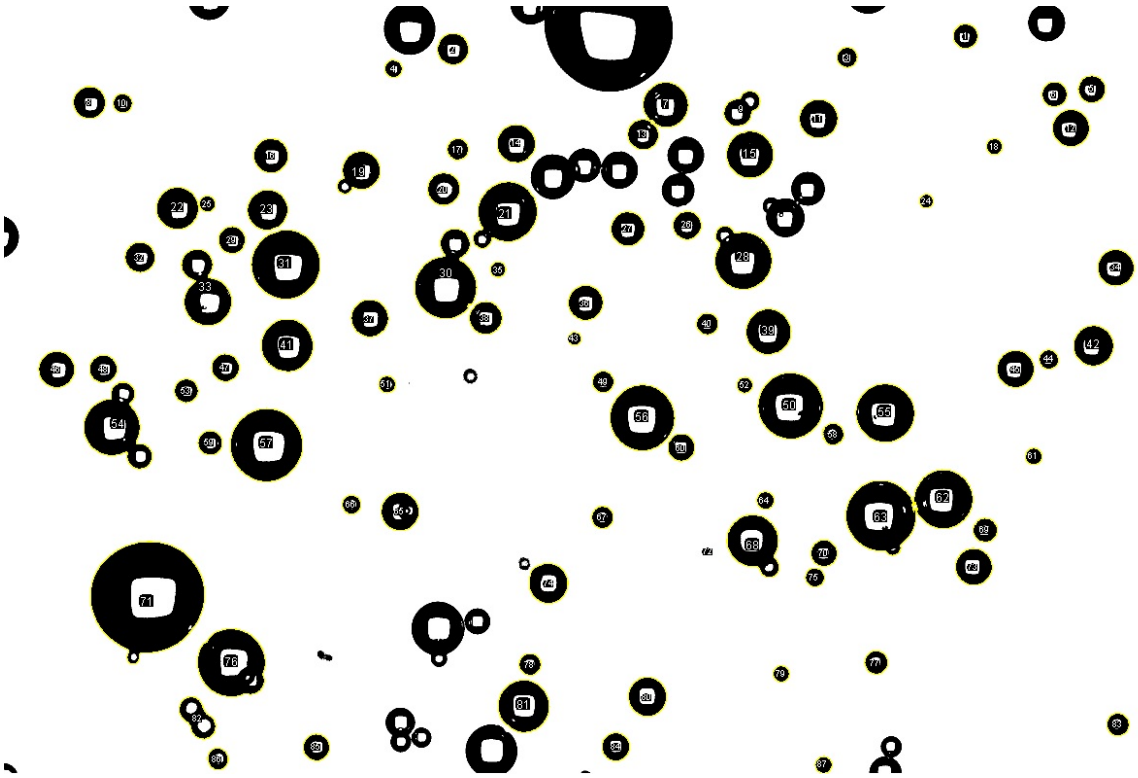

Figure 28: sample bubble picture, bubbles recognized and counted

This process excludes large clusters of bubbles and bubbles on the edge of pictures. As a result, the total measurement of this example picture is 87 bubbles counted.

There are two ways for the software to determine the bubble size after recognizing it as a valid bubble. The first is to measure it as a 2-dimensional ellipse, by determining the major and minor axes then computing the average diameter (e.g. d_{32}). The second way is to determine the area of the bubble then back-calculate the diameter considering it as a perfect circle. Since the bubble picture is essentially a projection of a sphere, both methods should result in similar estimates. However, considering the occasional clusters

of small bubbles being encountered and large bubbles with low circularity, the first calculation method was selected for this project. The results for this sample picture are: d_{10} equals to 0.69mm and d_{32} 1.09mm for the total 87 bubbles counted.

Both the bubble viewing equipment and the sizing technique utilized at McGill University is mature has proven reliable. The bubble viewer provides good lighting and clear images of the spread bubbles. With correct camera settings, the bubbles have distinct edges and good contrast.

4.3. Pressure and bubble size correction

Bubble sizes were corrected to a reference point. As shown in Figure 29, the reference point is at the level of the downcomer outlet, which is also the bubble viewer inlet as well as the middle point of the two differential pressure tabs. The difference in pressure between the reference point and where the bubbles are imaged requires that a

correction be made to bubble size to be consistent with the gas holdup measurement. The calculation is done as follows:

$$\mathbf{Pref} = \left(\mathbf{P} - \frac{\mathbf{DP}}{\mathbf{2}}\right) + \mathbf{Patm}$$

$$\mathbf{Ppic} = (\mathbf{Patm} + \mathbf{P} - \boldsymbol{\rho}\mathbf{gV}(\mathbf{H3} + \mathbf{H1}))$$

$$\mathbf{Dref} = \mathbf{Dpic} * \frac{\mathbf{Ppic}^{\left(\frac{1}{3}\right)}}{\mathbf{Pref}^{\left(\frac{1}{3}\right)}}$$

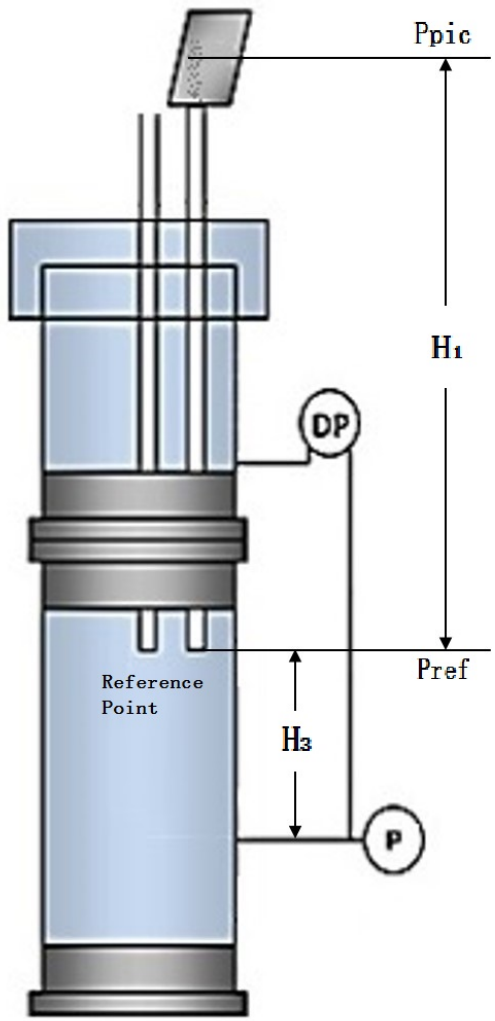

Figure 29: Bubble size correction calculation

Chapter 5: Results and Discussion

5.1. Vacuum Pressure and Working Condition of Downcomer

It has been established that certainly bubble regeneration and probably particle collection occurs in the downcomer. Establishing the necessary vacuum in the downcomer to achieve both is important and is controlled by various factors.

5.1.1. The effect of flowrate on vacuum pressure

The air and pulp flowrates are related to each other and have opposite effect on the vacuum pressure namely: when aeration rate increases the vacuum decreases; when pulp flowrate increases the vacuum increases. The air-to-pulp ratio (APR) is an important operating parameter. As shown in Figure 30, an increase of APR results in loss of vacuum. The experiment was conducted and repeated once under the same frother concentration (D250 30ppm) and same Jameson Cell geometrical setup. It can

be observed from this figure, though sharing similar trend, different pulp flowrates result in different rate of vacuum loss when APR changes.

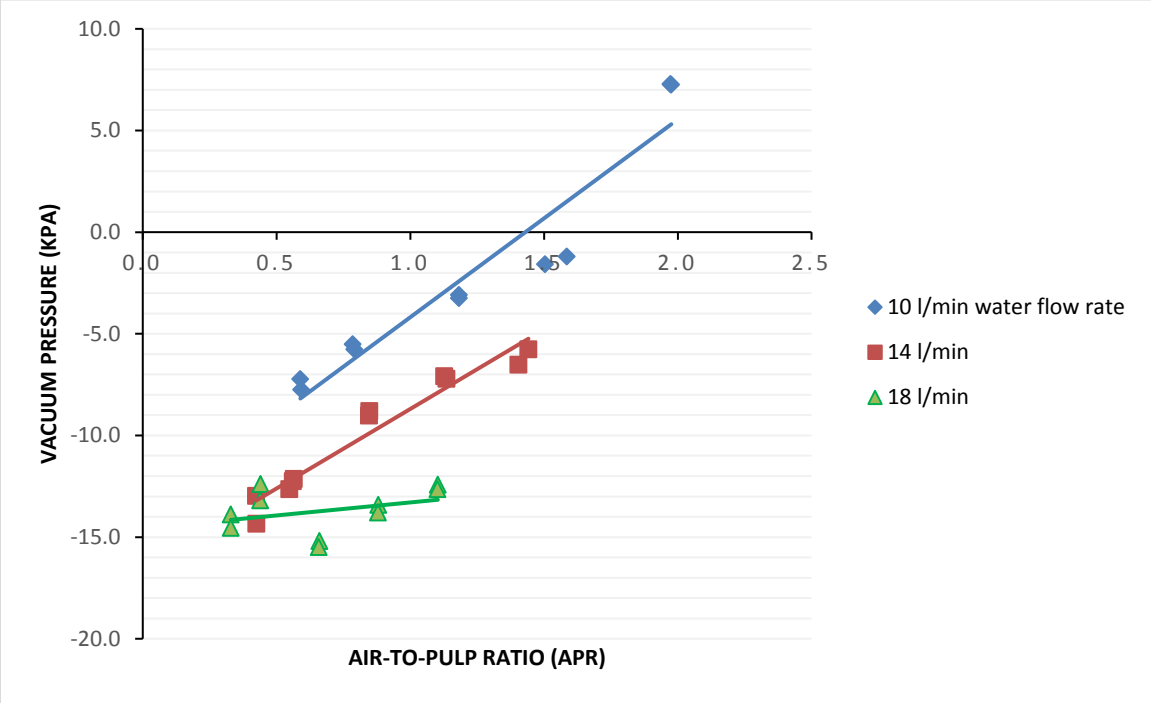

Figure 30: APR vs. vacuum pressure in an operating downcomer

Another representation of how APR affects the vacuum is shown in Figure 31. The red zone represents positive pressure zone, that is, where vacuum is lost. The vacuum gradient in the figure is approximately -1, but in most cases the vacuum pressure

gradient is not a constant. It represents how the vacuum changes for this specific Jameson Cell setup. There are also other parameters that affect the vacuum pressure.

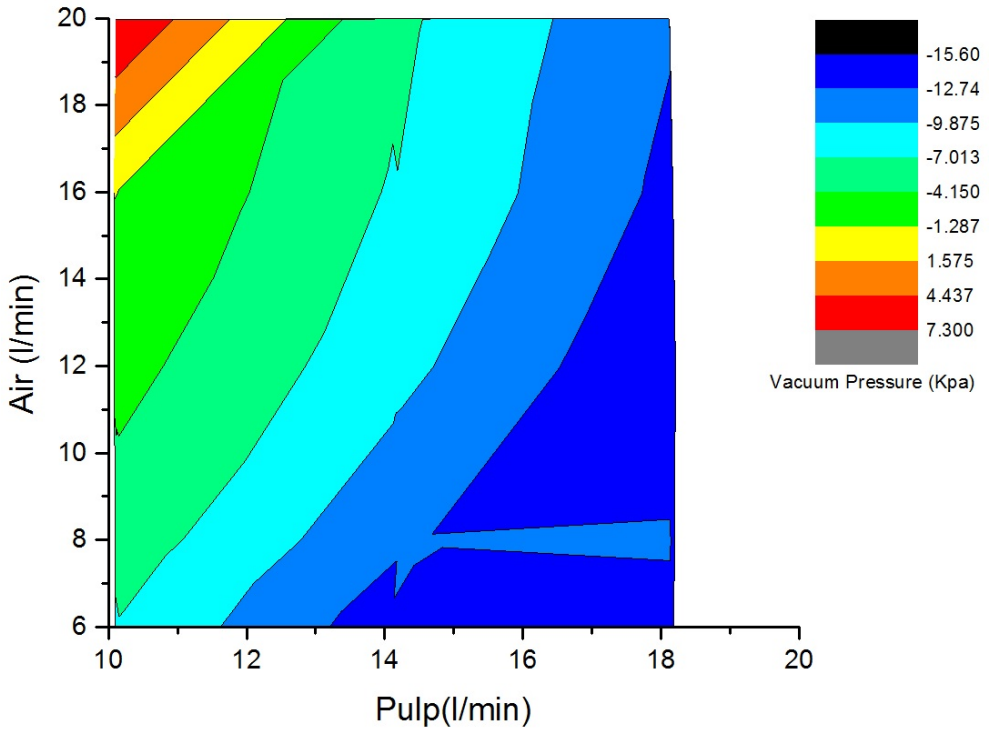

Figure 31: Contour diagram of APR effect on vacuum pressure

5.1.2. The Effect of Orifice Size on Vacuum Pressure

Even though the orifice plate is no longer the industrial choice, it continues to be a viable option at the lab scale because it can be readily changed. The orifice plate restricts the flow delivered to the downcomer creating the jet. Needless to say orifice geometry will have an effect on jet formation and thus an effect on the hydrodynamic

conditions in the downcomer. In this study, three sizes of orifice were tested: 4mm, 5mm and 6mm diameter.

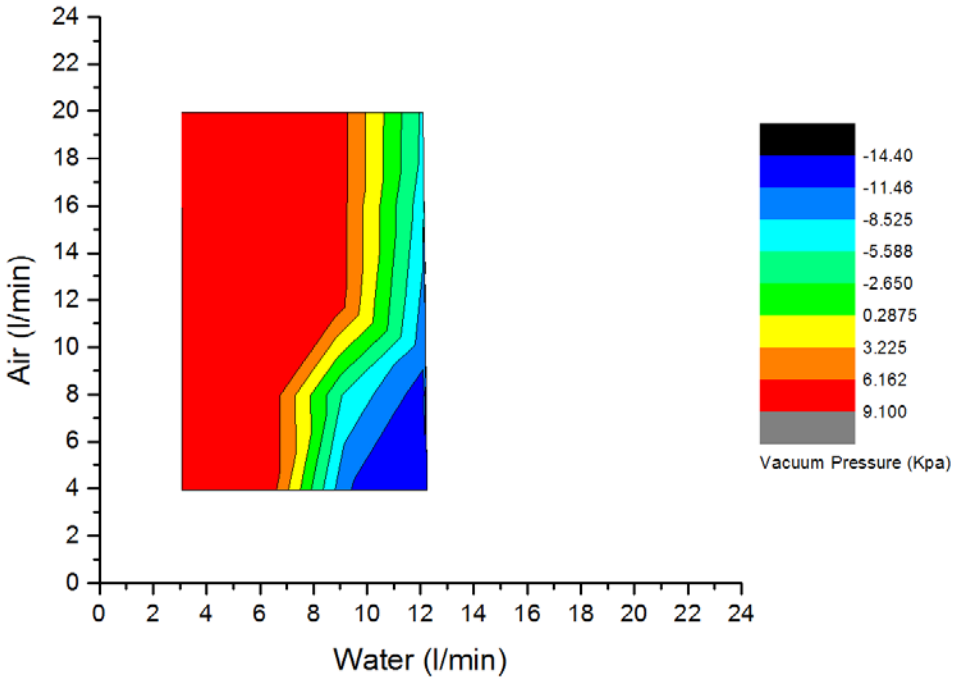

Figure 32: Contour diagram of APR effect on Vacuum Pressure: 4mm orifice

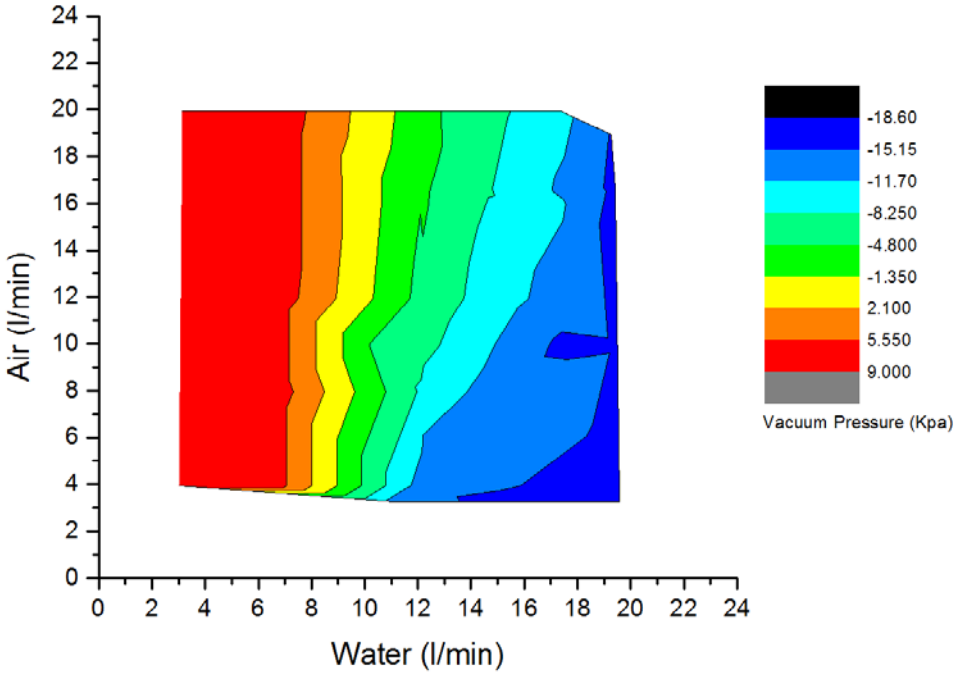

Figure 33: Contour diagram of APR effect on Vacuum Pressure: 5mm orifice

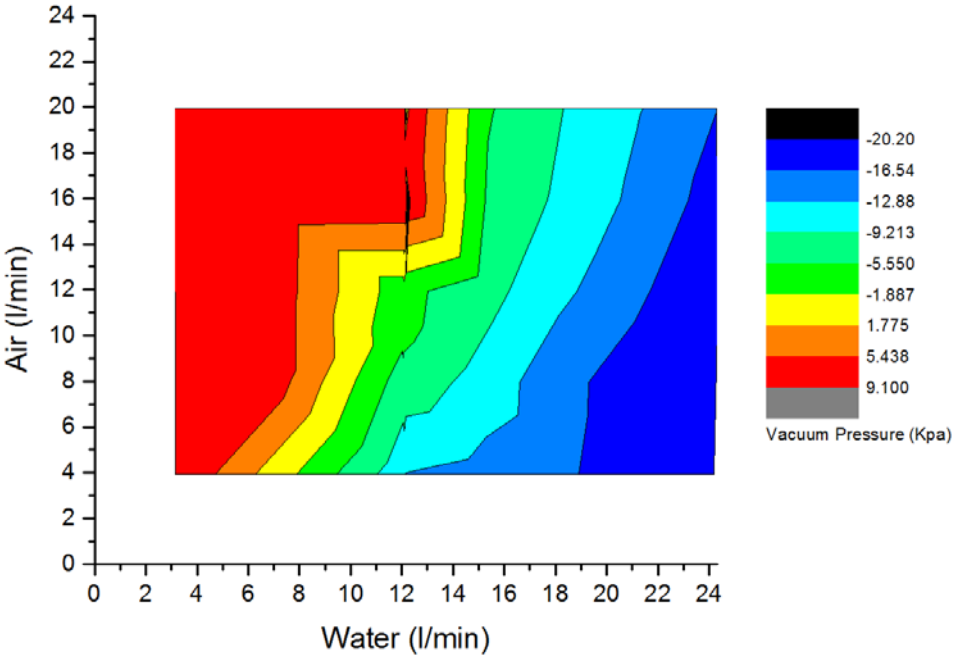

Figure 34: Contour diagram of APR effect on Vacuum Pressure: 6mm orifice

Figure 32, Figure 33 and Figure 34 show results of tests conducted at each orifice size as a function of flowrate and in the presence of 15ppm of DF250. Air flowrate was controlled by a PID controller and set to maximum at 20 L/min. For the 4, 5 and 6mm orifices, the corresponding maximum liquid flowrates were approximately 12, 20, 24 l/min, respectively. The orifice size also defines the minimum flowrate to generate the jet, which is around 8 L/min at the minimum air flowrate. This minimum could change if a different pump with different power output was used.

Loss of vacuum, that is, when vacuum pressure goes over zero, can be inferred from the figures to occur when APR is approximately equal to or greater than one. Conversely, when APR is less than one, vacuum is most often achieved, a result that seems independent of orifice size.

Lastly, the larger the orifice size, the higher the vacuum within the same operational limit. However this does not suggest the larger the orifice the better for the vacuum pressure, because if the orifice is too big for the pump to generate a jet with sufficient pressure it will compromise the mixing and bubble generation in the mixing zone.

5.1.3. The Effect of Downcomer Length on Vacuum Pressure

Downcomer length and exit depth relative to the separation tank are important designs variables that have received scant attention. According to the “kinetic” theory, a longer the downcomer would result in longer residence time and higher recovery. In this series of tests 3 lengths of downcomer at the same exit depth were used. At each downcomer length tests with different APR and frother concentration were used to determine the range of vacuum pressure that can be achieved. As Figure 35 shows, the

longer the downcomer the wider range of vacuum pressure it can support, and most importantly, the lower the vacuum pressure that can be achieved. Notably, it is not the downcomer length per se that results in higher vacuum, but the fact that the longer downcomer requires higher vacuum to allow the bubbly mixture height to reach closer to the top, resulting in longer mixing zone and pipe flow zone length.

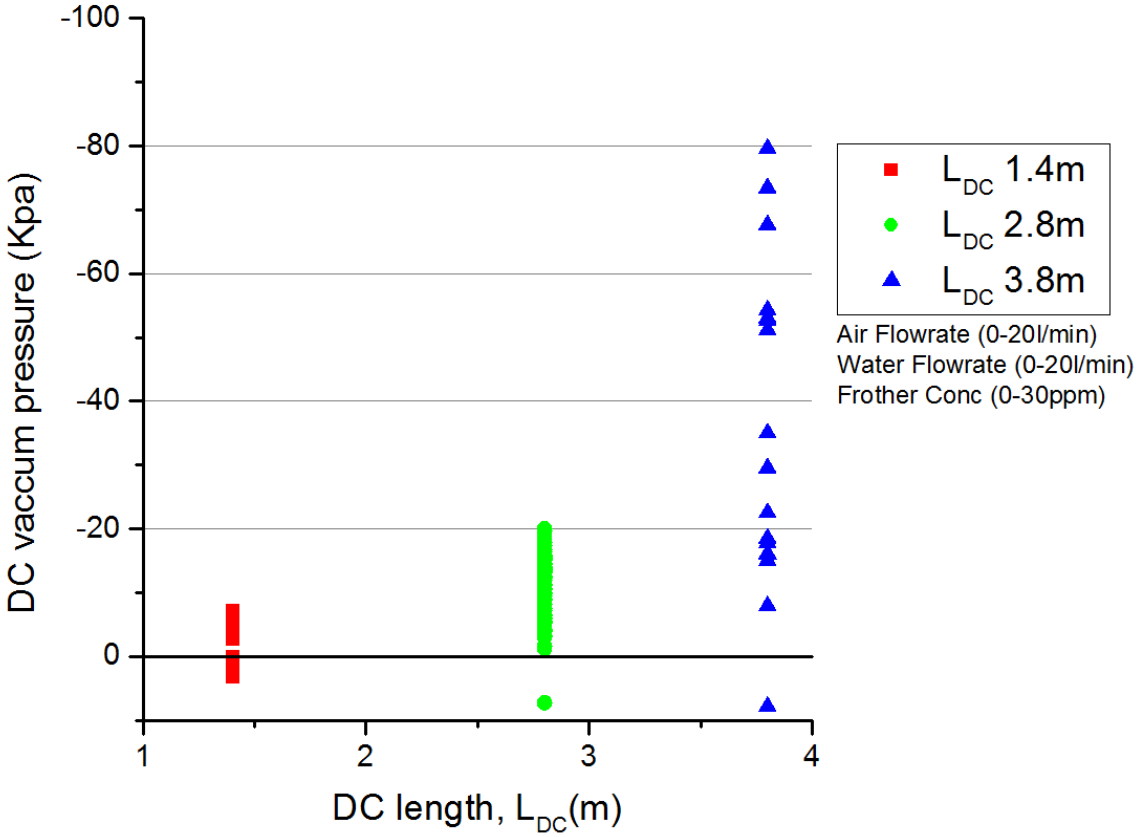

Figure 35: Effect of downcomer length on vacuum pressure

5.1.4. The Effect of Frother Concentration on Vacuum Pressure

Frother addition to the pulp significantly reduces the size of bubbles generated in any flotation machine, therefore increasing gas holdup and bubble surface area flux. In the case of the Jameson Cell, frother addition also enhances the vacuum by promoting air entrainment. Four sets of experiments were conducted with the same water flowrate, 20L/min, and gradually increasing frother (DF250) concentration (5, 10, 15, 30, 60ppm) at four aeration rates (3.3, 10, 16.6 and 25L/min). As Figure 36 shows, for otherwise the same operating conditions, the higher concentration of frother resulted in higher vacuum.

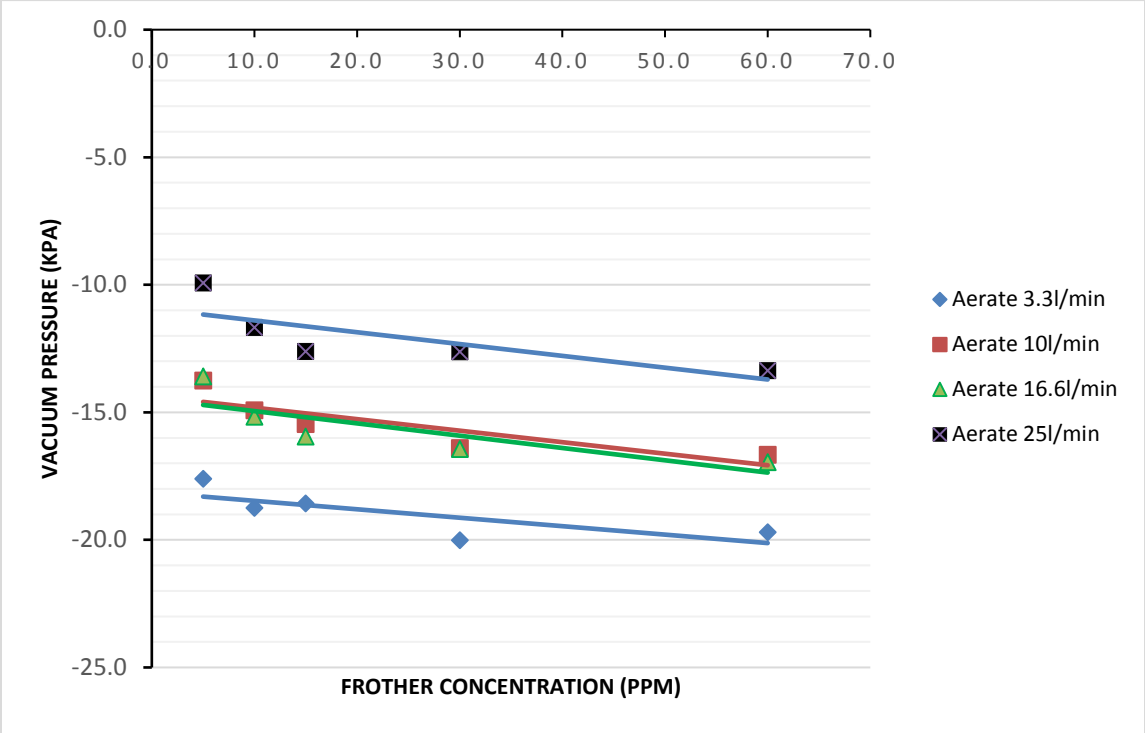

Figure 36: Frother effect on the vacuum pressure in downcomer

5.2. Jet pressure of Jameson Cell Downcomer

The pressure drop across the orifice plate ("jet pressure") was primarily determined by the system pump. However there are certain other aspects that influence the jet pressure, water flow rate and orifice size, for example, are significant. As Figure 37 demonstrates, at the same water flow rate the resulting jet pressure increased with decreasing orifice size. In Figure 38, the three downcomers of different length were tested over a range of operating conditions. According to the Student's t-test, the jet pressure generated by 1.4 and 2.8m lengths are not statistically different at the 95% confidence level. The downcomer length effect on the jet pressure, unlike its effect on the vacuum pressure, was minimal.

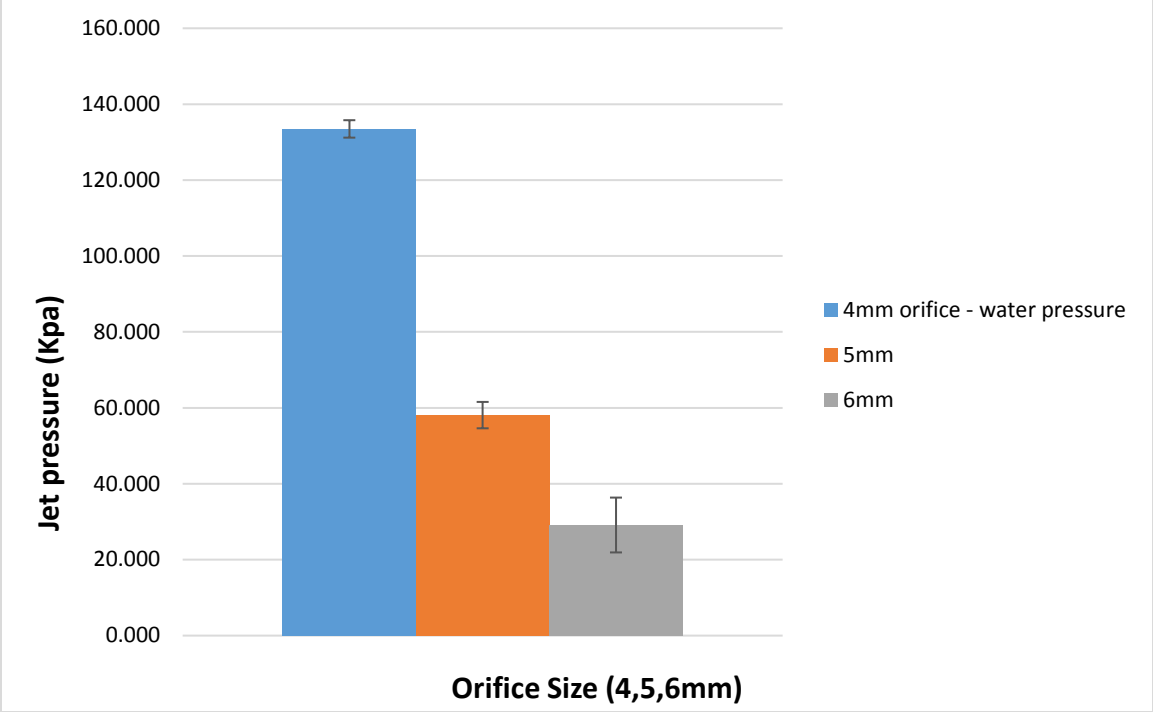

Figure 37: The effect of orifice size on the jet pressure

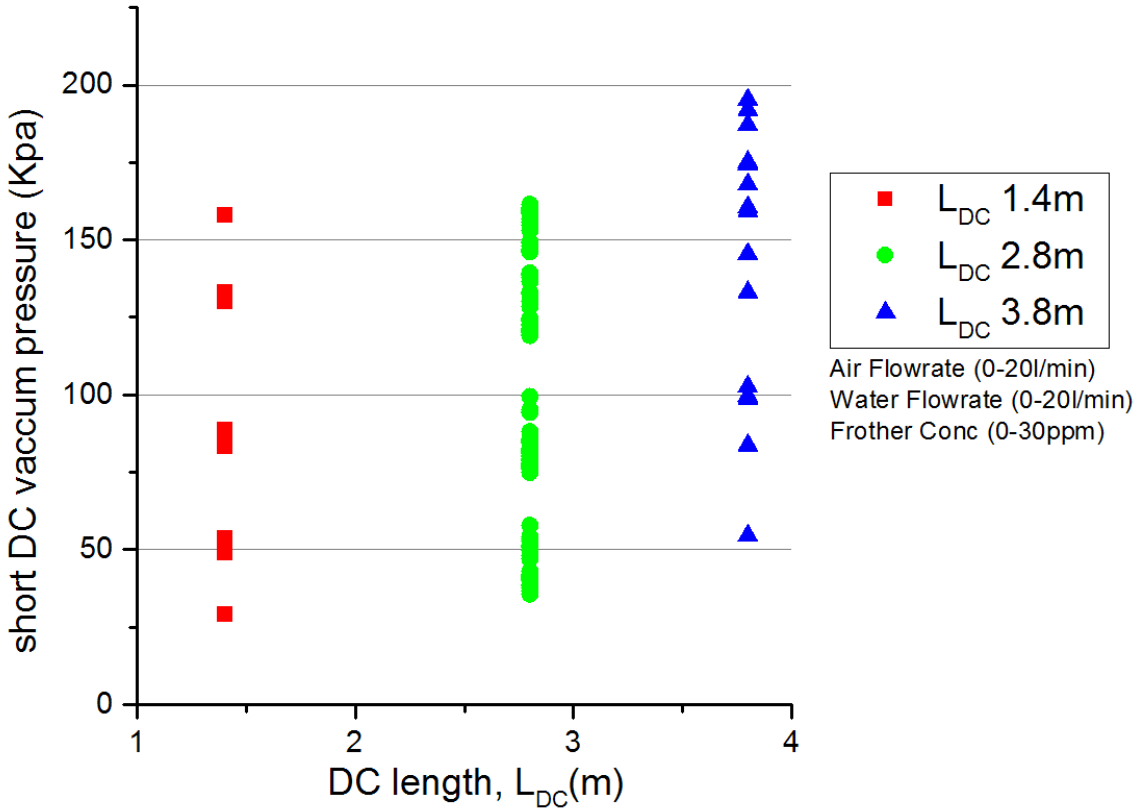

Figure 38: The effect of downcomer length on the jet pressure

5.3. Tank Gas Holdup

The gas holdup in the Jameson Cell is related to the bubble size and air-to-pulp ratio. Measuring the gas-holdup in the downcomer has been achieved using conductivity or pressure tapings along the downcomer [28]. The current setup does not have either feature. Gas holdup measured in this project is that in separation tank ("tank gas holdup"), which trends with the value in the downcomer. In mechanical cells and columns, under most operating conditions, increasing J_g will usually raise gas-holdup. However in the Jameson Cell this premise is predicated on there being a vacuum in the downcomer. As demonstrated in Figure 39, under that series of test conditions, increasing J_g over 0.6 m/s

resulted on losing vacuum (with the specific orifice and APR combinations). The consequence was that the gas holdup dropped significantly in the tank because losing the downcomer vacuum significantly increased the size of bubbles generated.

Tank gas holdup increases with increasing frother concentration, as shown in Figure 40. All tests in this series were within the 'normal' downcomer operating conditions, that is, vacuum was held. The higher the frother concentration, the higher the gas holdup. Pushing the J_g higher than common practice in industry and at high frother dosage, it is shown that the Jameson Cell can achieve fairly high gas holdup in tank, reflective of high gas holdup in the downcomer. A high tank gas holdup could be important as it may mean the tank functions as a second chance for particle collection.

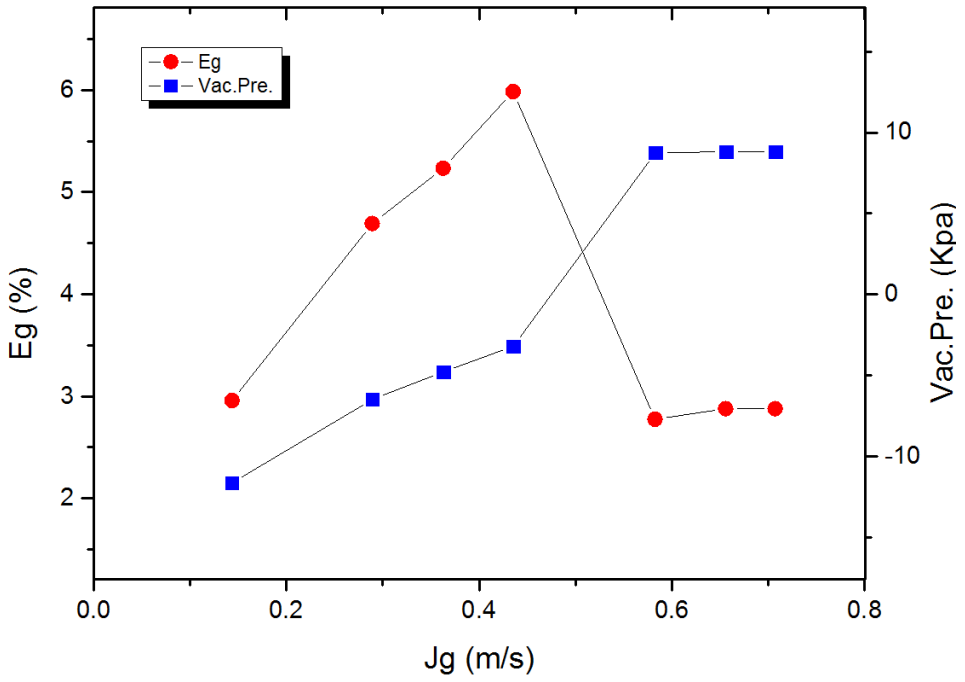

Figure 39: Gas holdup in separation tank is related to Jg and vacuum pressure

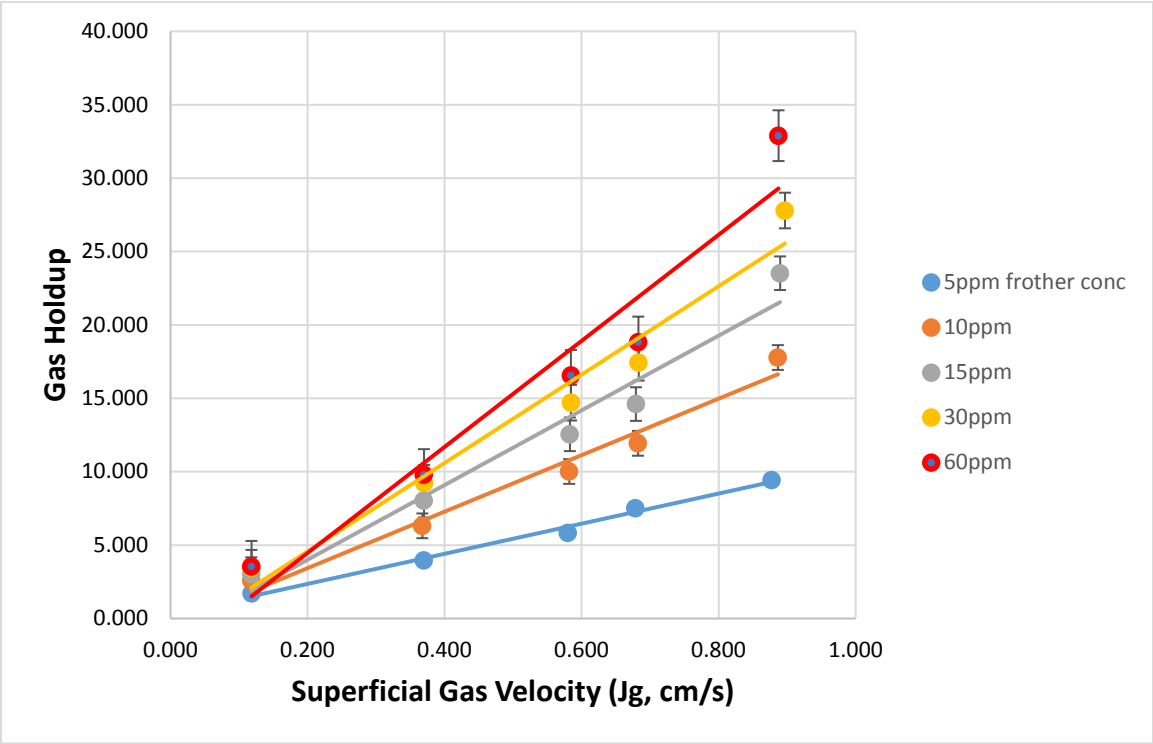

Figure 40: The effect of frother conc. on the tank gas holdup

5.4. Bubble Size

5.4.1. The Effect of Aeration Rate on Bubble Size

It is well established in all flotation machines that, all other factors held constant, increasing air flowrate increases gas holdup by introducing more bubbles, but, at the same time, increases the bubble size. The Jameson Cell too follows these trends. Air flowrate in the Jameson Cell is closely related to the vacuum pressure in the downcomer and is one of the primary variables that defines a Jameson Cell's working condition. The results in Figure 41are from two series of tests with the same frother concentration (DF250, 15ppm) and increasing air flowrate. They demonstrate that increasing air increased bubble size.

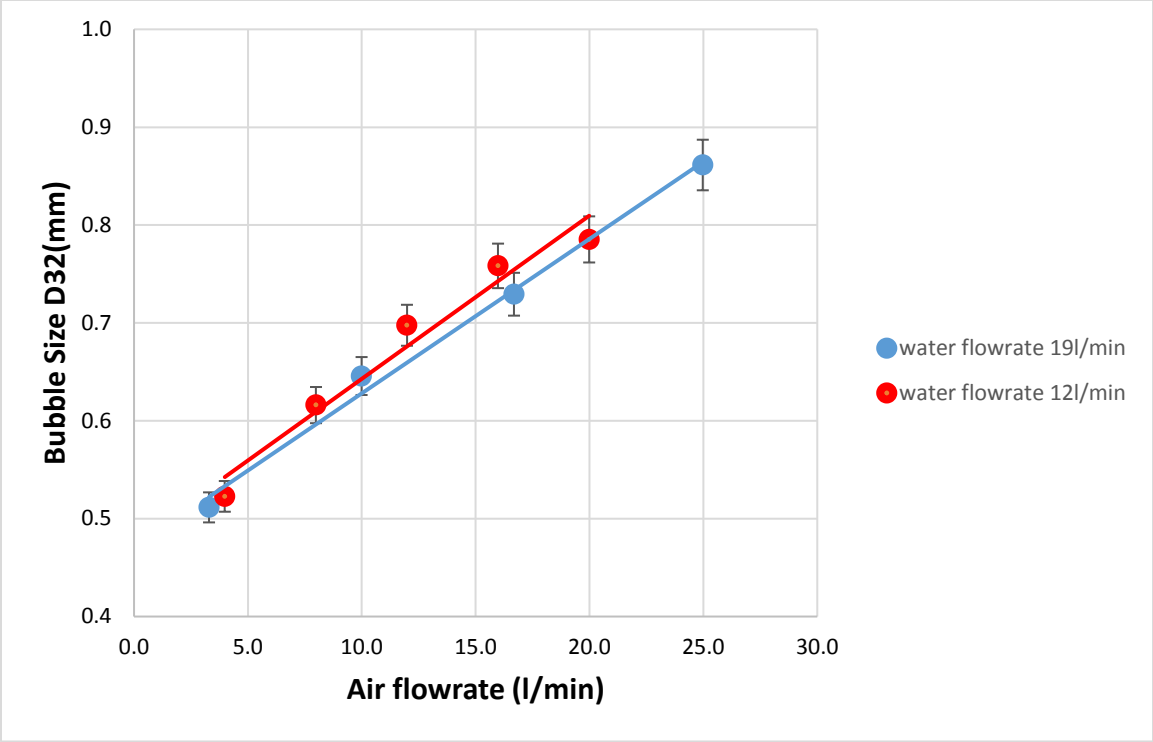

Figure 41: The effect of air flowrate on bubble size in Jameson Cell

5.4.2. The Effect of Water Flowrate on the Bubble Size and Its Implications

Increasing water flowrate, in contrast to air flow rate, decreases the bubble size. Increasing water flowrate reduces the APR which generally yields smaller bubble size. Figure 42 shows the results of experiments conducted at the same frother condition (DF250, 30ppm) at three set air rates and increasing water flowrate. The effect of

increasing water flowrate on decreasing bubble size is significant. Figure 42 also reminds that high air flowrate promotes large bubble size.

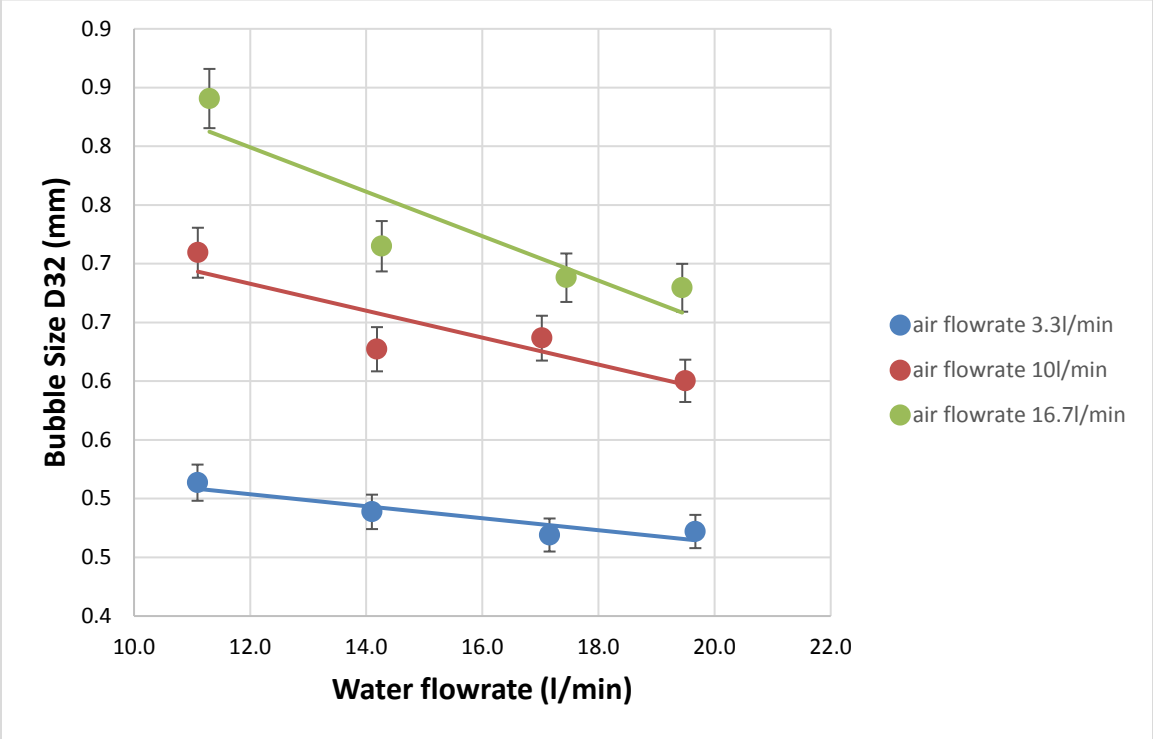

Figure 42: The effect of water flowrate on bubble size in Jameson Cell

Many operators maintain that the APR is important as a criterion for defining the operating condition. However, as the previous chapter proposed, air-to-pulp ratio is a secondary variable and its effects are the result of either air and water flowrate interaction or the vacuum and jet pressure interaction. To demonstrate this, the following experiments were conducted with air-to-pulp ratio held equal to one. At the three frother concentrations used, 10, 15, and 30ppm, Figure 43 shows that bubble size decreases as flowrate (air = water) is increased. There is a tendency for effects to cancel as flowrate is increased, the increase in air increasing bubble size while increase in water

decreasing bubble size. As Figure 40 indicates the offset is not exact and it appears that water flowrate, perhaps by influencing jet pressure, has the stronger effect. This result can be explained by the plunging jet generating bubbles through dissipation of its kinetic energy.

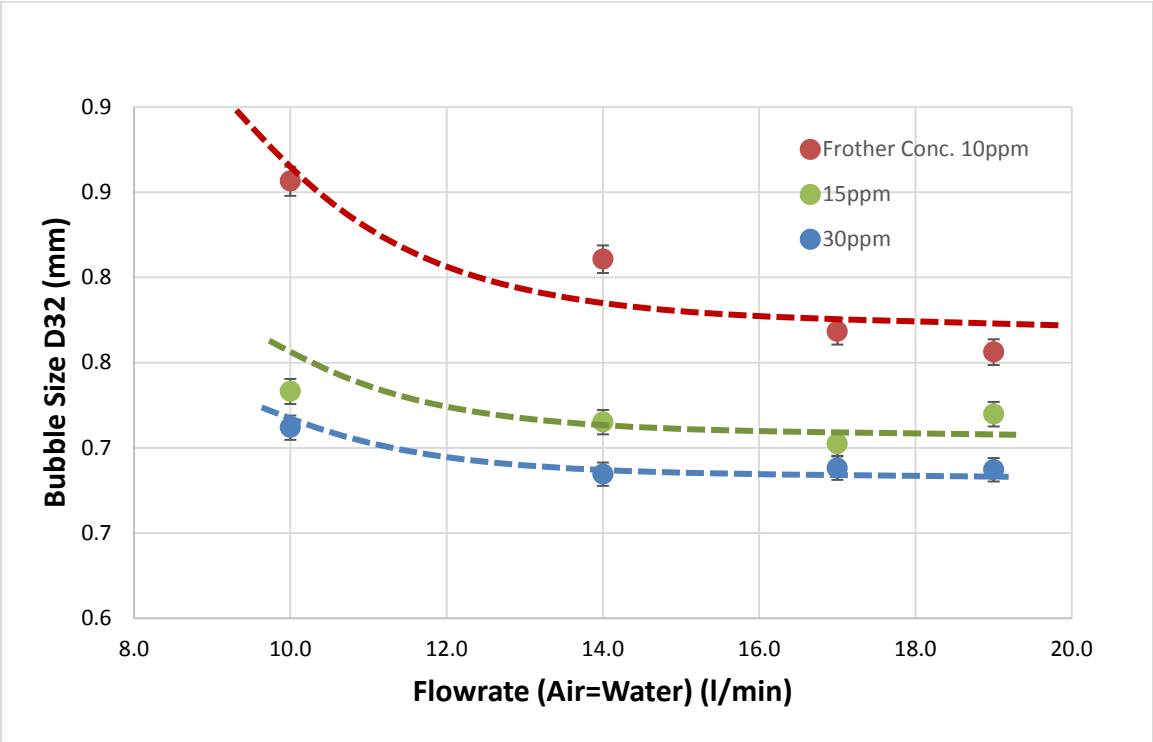

Figure 43: Flowrate vs. bubble size (under APR=1 condition)

5.4.3. The Effect of Frother on the Bubble Size

Frother's effect in reducing bubble size in flotation machines is well known and the Jameson Cell is no exception. Reducing bubble size through frother addition results in a series of changes in Jameson Cell operation, for example, vacuum pressure changes, and gas hold up (both in downcomer and tank) changes. These changes will lead to further influences such as longer residence time and deeper froth height. To demonstrate

the frother effect on bubble size, Figure 44 to 48 show the bubble size profile for L_{DC} 2.8m and 5mm orifice diameter. (Note, 20 L/min of air flowrate is approximately 0.7 cm/s in the tank and 50cm/s in the downcomer.)

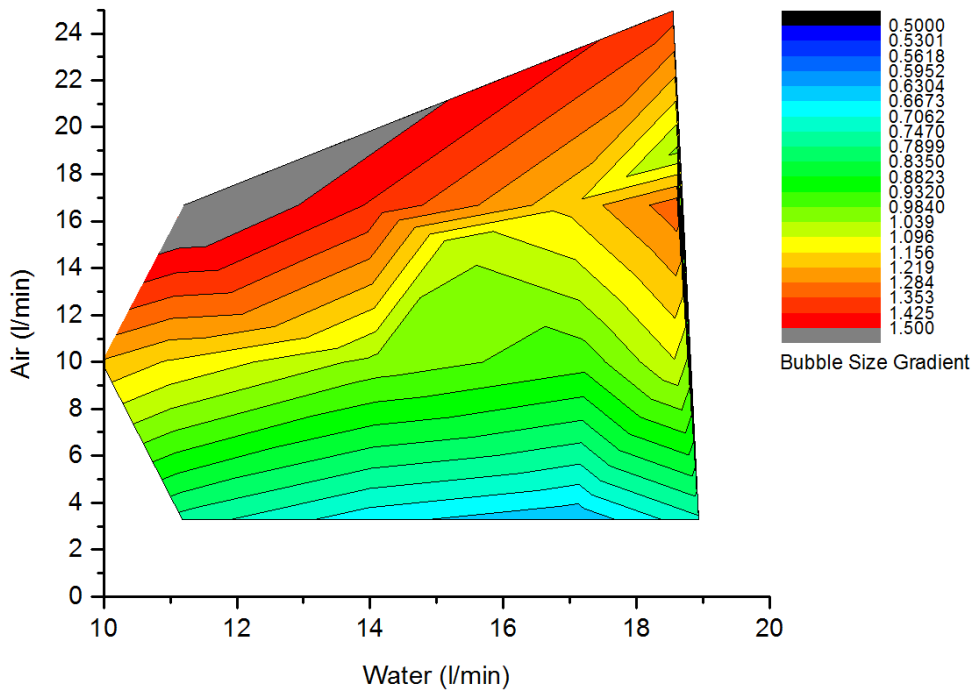

Figure 44: Bubble size profile: 5ppm frother

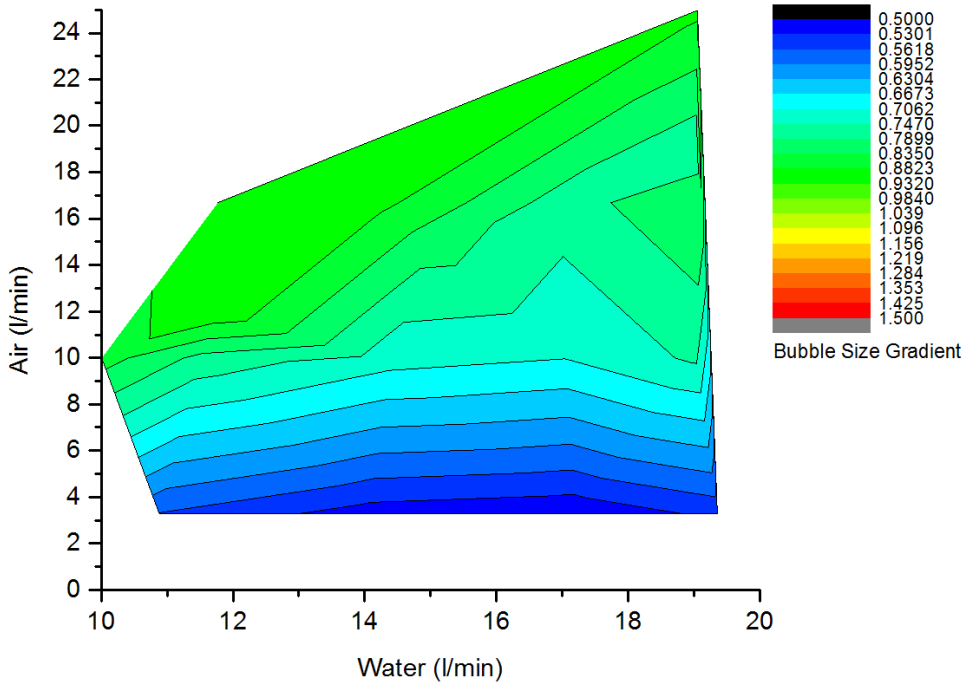

Figure 45: Bubble size profile: 10ppm frother

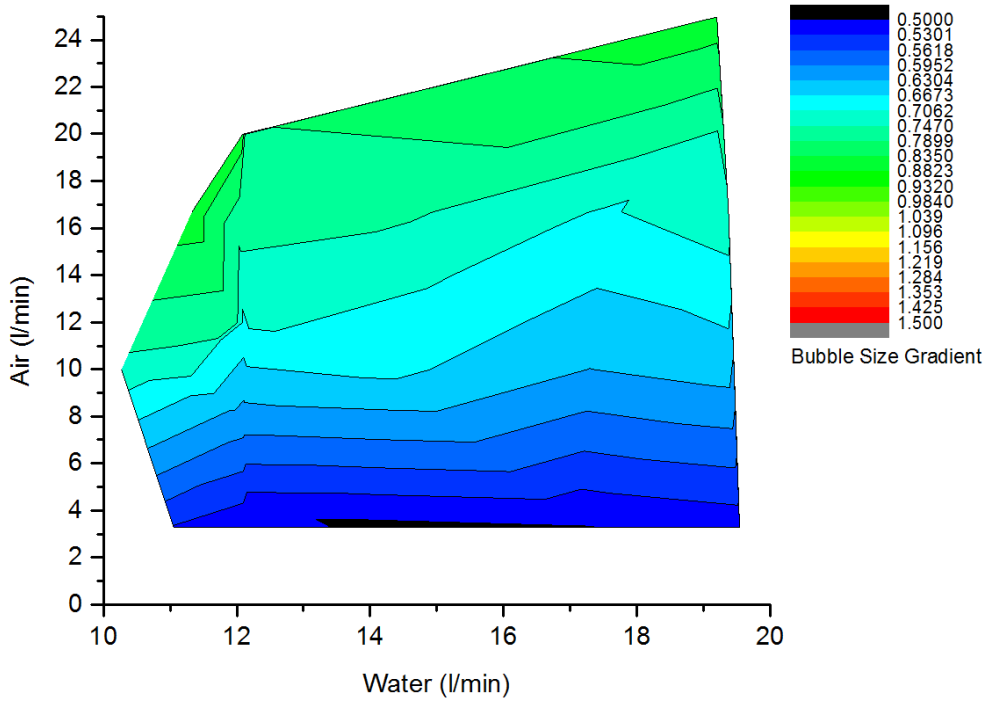

Figure 46: Bubble size profile: 15ppm frother

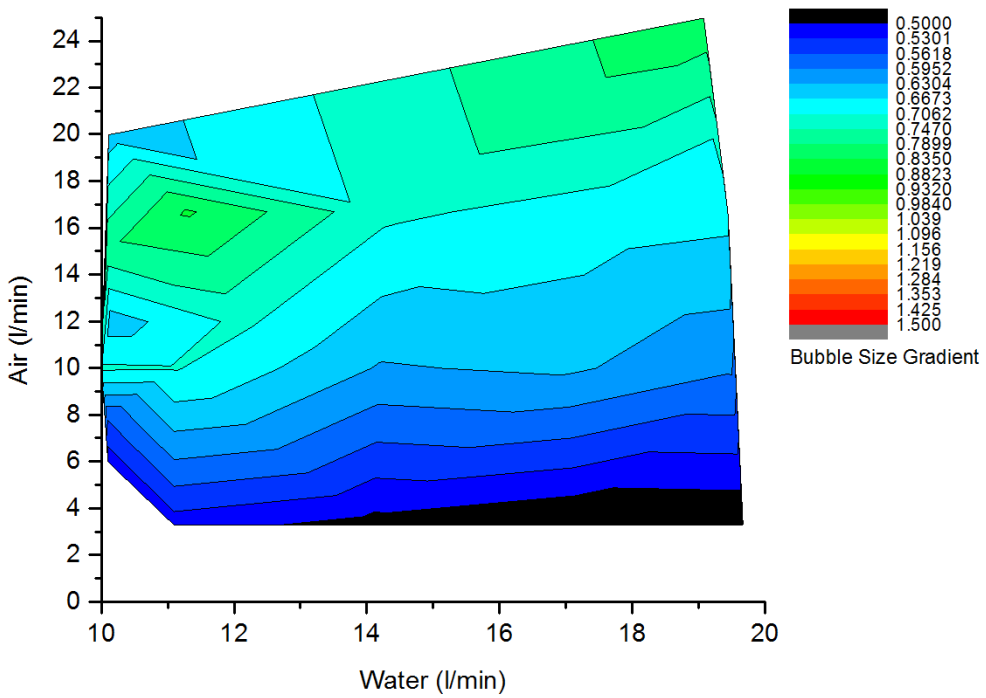

Figure 47: Bubble size profile: 30ppm frother

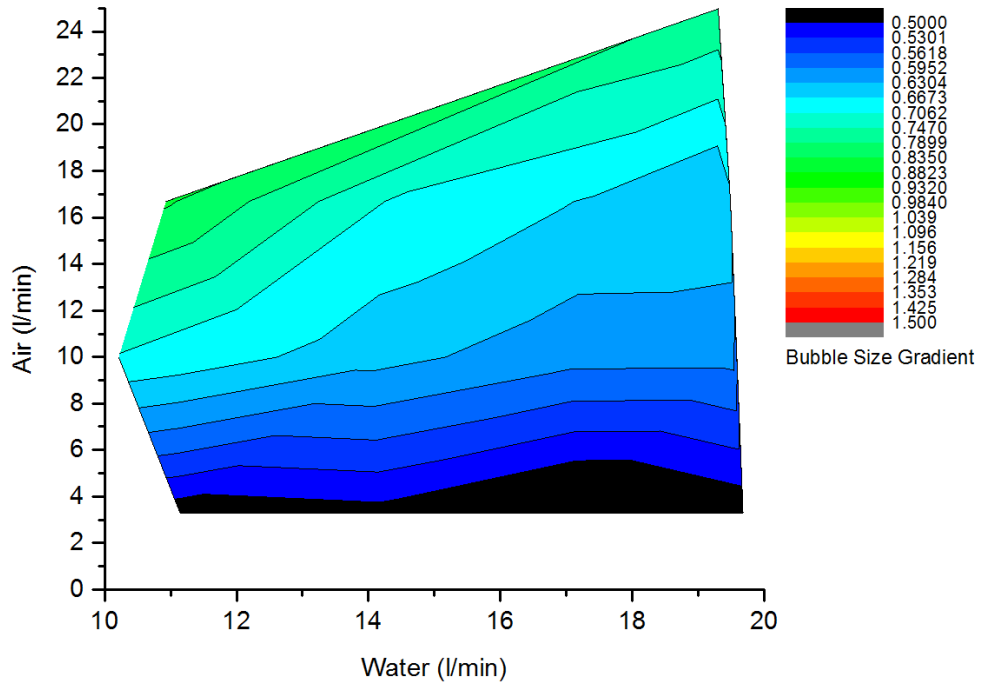

Figure 48: Bubble size profile: 60ppm frother

From the bubble size profiles, small bubble (<600um) generation occurs in the low APR region regardless of frother concentration. Over-dosing frother could result in small bubbles even when high APR conditions are used; however, the effect of frother on bubble size starts diminishes after ca. 8ppm, that is, the approximate CCC (critical coalescence concentration) for DF250 in this Jameson Cell.

5.4.4. The Effect of Jameson Cell Geometry on the Bubble Size

Aspects of the geometry were introduced in chapter 2. The geometry variables studied in this project were orifice size and downcomer length. Orifice size is directly related to the jet pressure and therefore its effect on the bubble size has already been discussed. Two sets of experiments with identical operating conditions were conducted using both a short and long downcomer (1.4m and 3.8m). Bubble sizes collected at the same exit level in both cases displayed no significant difference, as shown in Figure 49 where most bubble sizes measured are within 10% for each length. Even though

downcomer length plays no significant role in bubble size, it is important in residence time which could affect particle collection.

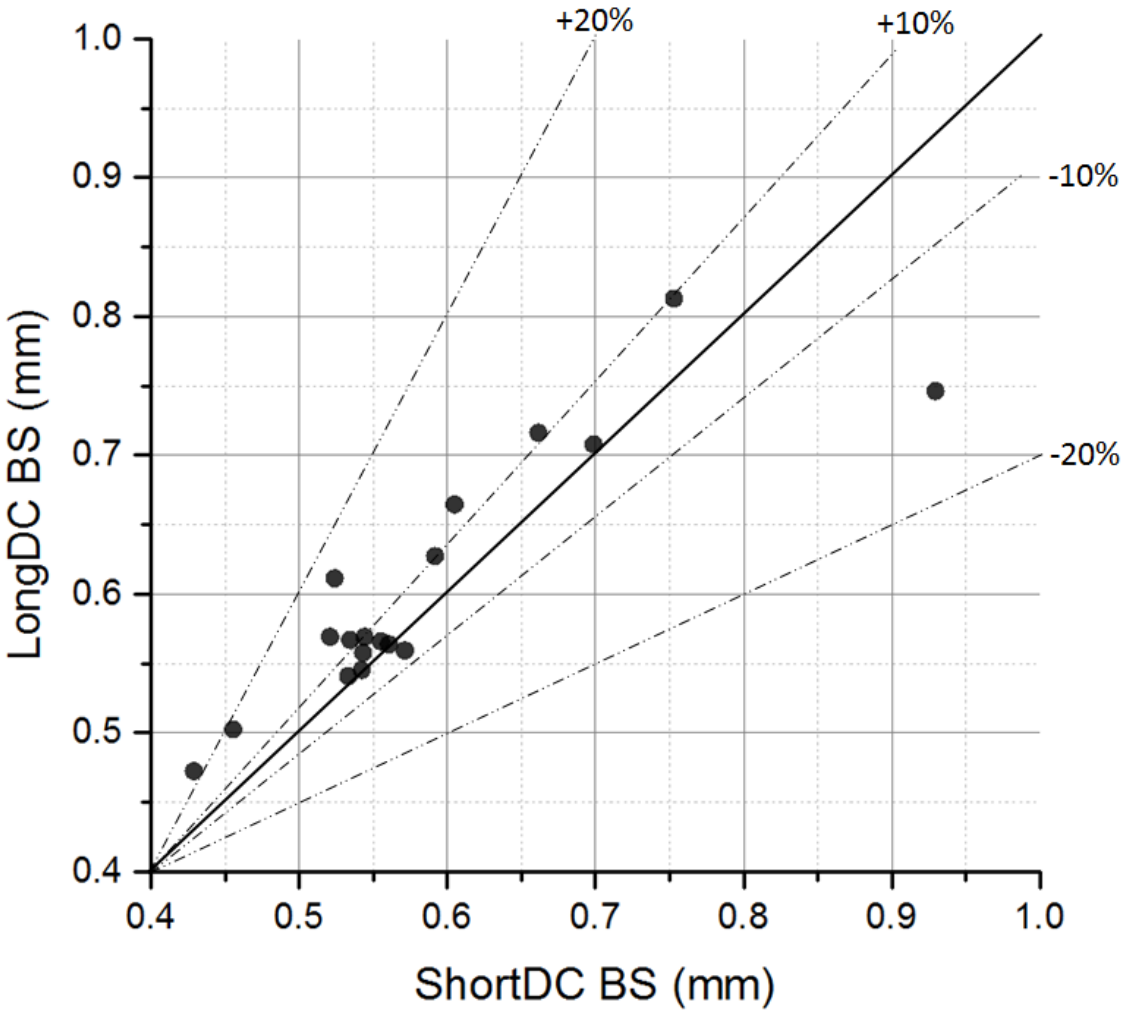

Figure 49: Comparison of bubble size generated by long and short downcomer

Chapter 6: Conclusions and Future Work

The effect of and interaction among operating and design variables of the Jameson Cell on the downcomer operating condition and bubble size were investigated in this thesis.

The primary variables that are intrinsic and have the stand-alone influence on the performance of Jameson Cell are its geometrical design (orifice, downcomer, tank dimensions), properties of the fluid (air and slurry), and feed pressure. Secondary variables are derived from the primary ones, for example, J_g (superficial gas velocity), gas holdup and recovery. Jameson Cell operation involves many variables and knowing which intrinsic ones are the most important is critical.

The optimum Jameson Cell working condition is when the downcomer retains vacuum and the contact surface of plunging jet and slurry is significantly above the tank slurry level. Liquid flowrate negatively impacts downcomer vacuum while the addition of frother promotes vacuum. In terms of the Jameson Cell design variables, both the orifice size and downcomer length positively impact the vacuum. A good vacuum condition promotes small bubbles and high gas holdup, which usually favor increased particle collection rates.

Bubble size is another important aspect studied in this thesis. Air and slurry flowrate have opposite effects on size of bubbles generated in the Jameson Cell. In most cases, the lower the APR (air to pulp ratio), the smaller the bubble size. Interestingly, this study has also shown that higher jet pressure helps to generate smaller bubbles. It has also been demonstrated that the downcomer length does not have a significant effect on bubble size.

Suggestions for future work have two general directions. The first is to study the plunging jet mechanism, establishing the relationship between gas dispersion and the

plunging liquid jet reactor condition. Many researchers have attempted to mathematically describe the fluid dynamics of the downcomer, the most significant being the prediction of bubble size treating the problem as that of the plunging liquid jet reactor.

The other direction is more practical, to extend the present study to include particle recovery under different design and operating conditions in a Jameson cell.

References

1. Finch, J.A. and B.A. Wills, *Wills' Mineral Processing Technology: An Introduction to the Partical Aspects of Ore Treatment and Mineral Recovery*. 8th ed. 2015: Butterworth-Heinemann.
2. Cowburn, J.A., et al. *Design developments of the Jameson Cell*. in *Proc. Centenary of Flotation Symp.* 2005. Brisbane, Australia.
3. Evans, G.M., B.W. Atkinson, and G.J. Jameson, *The Jameson Cell*. 1995, University of Newcastle: Newcastle, New South Wales, Australia.
4. Taggart, A.F., *Handbook of Mineral Processing*. 1927, New York: Wiley.
5. Espinosa-Gomez, R., et al.,, *Coalescence and froth collapse in the presence of fatty acid.* Colloids Surf., 1988. **32**: p. 197-209.
6. Harbort, G.J., *Recent advances in Jameson Flotation cell technology.* Minerals Engineering, 1994. **7**(2/3): p. 319.
7. Osborne, D., et al. *Two decades of Jameson Cell installations in coal*. in *XVII. International Coal Prepartion Congress*. 2013. ISTANBUL TURKEY: Xstrata Technology.
8. Glencore, *Jameson Cell Rising To The Challenge*, Xstrata, Editor. 2014. p. 2.
9. Jameson, G.J., G.J. Harbort, and N. Riches, *The Development and Application of the Jameson Cell*, in *4th Mill Operators' Conference*. 1991, AusIMM: Melbourne. p. 45-50.
10. Murphy, A., S,, et al. *Breaking the Boundaries of Jameson Capacity*. in *The Eighth Australian Coal Preparation Conference, ACPS*. 2000. Nelson Bay, New South Wales.
11. Evans, G.M., G.J. Jameson, and B.W. Atkinson, *Prediction of The Bubble Size Generated by A Plunging Liquid Jet Bubble Column.* Chem. Eng. Sci., 1992. **47**: p. 3265-3272.
12. Evans, G.M. and G.J. Jameson, *Free Jet Expansion and Gas Entrainment Characteristics of a Plunging Liquid Jet.* Experimental Thermal and Fluid Science, 1996. **12**: p. 142-149.
13. Lange, V., B.J. Azzopardi, and P. Licence, *Hydrodynamics of Ionic Liquids in Bubble Columns*, in *Ionic Liquids - New Aspects for the Future*, J.-i. Kadokawa, Editor. 2013. p. 143-163.
14. Langberg, D.E. and G.J. Jameson, *The coexistence of the froth and liquid phases in a flotation column.* Chem. Eng. Sci., 1992. **47**(17-18): p. 4345-4355.
15. Hinze, J.O., *Fundamentals of the hydrohynamic mechanism of splitting in dispersion processes.* AIChE. J., 1955. **1**: p. 289-295.
16. Cunningham, R.G., *Gas compression with the liquid jet pump.* J. Fluids Eng., 1974. **3**: p. 203-215.
17. Ryskin, G. and L.G. Leal, *Numerical solution of free-boundary problems in fluid machanics. Part 3. Bubble deformation in an axisymmetric straining flow.* J. Fluids Mech., 1984: p. 37-43.
18. Tasdemir, T., B. Oteyaka, and A. Tasdemir, *Air entainment rate and holdup in the Jameson Cell.* Mineral Engineering, 2007. **20**: p. 761-765.
19. Tasdemir, A., T. Tasdemir, and B. Oteyaka, *The effect of particle size and some operating parameters in the separation tank and the downcomer on the Jameson Cell recovery.* Minerals Engineering, 2007. **20**: p. 1331-1336.
20. Finch, J.A. and G.S. Dobby, *Column Flotation*. 1st ed. 1990: Permagon Press: Oxford.
21. Jameson, G.J. and E.V. Manalapig. *Flotation Cell Design-Experiences with the Jameson Cell*. in *AusIMM Extractive Metallurg Conference*. 1991.
22. Gomez, C.O. and J.A. Finch, *Gas dispersion measurements in flotation machines.* International Jornal of Mineral Processing, 2007. **84**: p. 51-58.

23. Marchese, M.M., et al.,, *Measurement of gas holdup in a three-phase concurrent downflow column.* Chem. Eng. Sci., 1992. **47**: p. 3475-3482.
24. Jameson, G.J., *Jameson flotation column operation manual*. 1990, University of Newcastle, Australia.
25. L. Huynh, et al., *Design And Performance Aspects of Coal Flotation - Experiences with The Jameson Cell*. 2012, Xstrata Technology, Australia.
26. Yoon, R.H. and G.H. Luttrell, *The effect of bubble size on fine particle flotation.* Mineral Processing and Extractive Metallurgy Review: An International Journal, 2007. **5**(1-5): p. 101-122.
27. Harbort, G.J., E.V. Manlapig, and S.K. DeBono, *Particle collection within the Jameson cell downcomer.* Trans. Instn Min. Metall. (Sect. C: Mineral Process. Extr. Metall.), 2002. **111**.
28. Cortes-Lopez, F., *Design of a Gas Holdup Sensor For Flotation Disgnosis*, in *Department of Mining and Matallurgical Engineering*. 1998, McGill University: Montreal, Canada.